Hyperspectral Remote Sensing of the Coastal Ocean: Adaptive Sampling and Forecasting of Near-Shore In Situ Optical Properties

W. Paul Bissett
Florida Environmental Research Institute
4807 Bayshore Blvd.
Suite 101
Tampa, FL 33611
phone: (813) 837-3374 x102   fax: (813) 902-9758   email: pbissett@feriweb.org

LONG-TERM GOALS

Water clarity is a key parameter of coastal ecology, as well as being important to some near-shore Naval operations. The clarity of the water column depends upon the depth-dependent distribution of the inherent optical properties and the geometric structure of the light field (an apparent optical property). Our long-term goal is to develop the remote sensing techniques, data analysis, and modeling capabilities to nowcast and forecast the 3-dimensional Inherent and Apparent Optical Properties (IOPs and AOPs) of the near-shore coastal environment.

(This report is the Final Report of Co-Principal Investigator, W. P. Bissett, to a larger program led by O. Schofield, Rutgers University, Award N00014-99-1-0196. It was given a no-cost extension for the first quarter of 2005, and is included here in its entirety.)

OBJECTIVES

1) To develop and deploy optical systems in the coastal ocean to create in-water optical products from remote sensing imagery.

2) Reformulate 1-dimensional Ecological Simulation 1.0 into 3-dimensional simulation of the coastal IOPs and AOPs, and couple this new code with the Regional Ocean Modeling System (ROMS) being developed at Rutgers University.

3) Develop the techniques to incorporate IOPs measured from in situ and estimated from remote sensing data, into a 3-dimensional nowcast/forecast model of the Long-term Ecological Observatory at 15 meters (LEO-15) off the coast of New Jersey.

APPROACH

The abilities to identify bathymetry, submerged obstacles, bottom type, or water clarity are clearly required for Mine Warfare (MIW), Mine Counter Measures (MCM), and Naval Special Warfare (NSW), particularly in the Very Shallow Water (VSW), riverine and estuarine environments. These requirements may be satisfied by 1) in-water systems that measure the properties of interest directly, i.e. multibeam sonar and laser-line scanners, 2) estimates from inversion of remote sensing data, or 3)

1. REPORT DATE **30 SEP 2005**	2. REPORT TYPE	3. DATES COVERED **00-00-2005 to 00-00-2005**

4. TITLE AND SUBTITLE **Hyperspectral Remote Sensing of the Coastal Ocean: Adaptive Sampling and Forecasting of Near-Shore In Situ Optical Properties**	5a. CONTRACT NUMBER
	5b. GRANT NUMBER
	5c. PROGRAM ELEMENT NUMBER
6. AUTHOR(S)	5d. PROJECT NUMBER
	5e. TASK NUMBER
	5f. WORK UNIT NUMBER

7. PERFORMING ORGANIZATION NAME(S) AND ADDRESS(ES) **Florida Environmental Research Institute,4807 Bayshore Blvd, Suite 101,Tampa,FL,33611**	8. PERFORMING ORGANIZATION REPORT NUMBER

9. SPONSORING/MONITORING AGENCY NAME(S) AND ADDRESS(ES)	10. SPONSOR/MONITOR'S ACRONYM(S)
	11. SPONSOR/MONITOR'S REPORT NUMBER(S)

12. DISTRIBUTION/AVAILABILITY STATEMENT
Approved for public release; distribution unlimited

13. SUPPLEMENTARY NOTES
code 1 only

14. ABSTRACT

Water clarity is a key parameter of coastal ecology, as well as being important to some near-shore Naval operations. The clarity of the water column depends upon the depth-dependent distribution of the inherent optical properties and the geometric structure of the light field (an apparent optical property). Our long-term goal is to develop the remote sensing techniques, data analysis, and modeling capabilities to nowcast and forecast the 3-dimensional Inherent and Apparent Optical Properties (IOPs and AOPs) of the near-shore coastal environment.

15. SUBJECT TERMS

16. SECURITY CLASSIFICATION OF:			17. LIMITATION OF ABSTRACT	18. NUMBER OF PAGES	19a. NAME OF RESPONSIBLE PERSON
a. REPORT **unclassified**	b. ABSTRACT **unclassified**	c. THIS PAGE **unclassified**	**Same as Report (SAR)**	**34**	

forecasts from 4-D environmental models. The focus on optical measures rather than acoustic measures allows for the estimation of these environmental characterizations, and target detection (e.g. Mine-Like Objects for MCM), from larger stand-off distances in access denied areas via remote sensing on aircraft and spacecraft platforms. Optical properties are also well suited for rapid environmental assessment, as the instrumentation to measure absorption, attenuation, and water-leaving radiance are better engineered and more stable than those systems to determine chlorophyll biomass, which has been a traditional proxy for optical clarity. In addition to the Naval uses, optics could become a better proxy for ecosystem health for coastal resource managers, since these parameters can be more quantitatively described, with instrumentation that is more robust. Thus, sampling and modeling of the optical properties of the coastal zone would be a boon to environmental resource managers, as well as those Naval operations that depend upon water clarity, bathymetry, bottom typing, target detection, and performance prediction modeling.

The breath of area, as well as the rapid change of the water conditions in the coastal ocean makes any sampling, optical or otherwise, very time consuming and difficult. However, the focus on optics allows us to explore remote sensing techniques that can rapidly sample large areas, either by aircraft or satellite sensors. Optical remote sensing techniques have generally relied on empirical methods to invert the water-leaving radiance signal to relative measures of optical constituents, e.g. chlorophyll a (Gordon and Morel, 1983), or apparent optical properties, e.g., diffuse attenuation coefficients (Austin and Petzold, 1981). These inversion techniques assume a homogenous optical layer and were developed mainly for open ocean conditions. Thus, they have difficulties in more turbid coastal waters. Other techniques have been developed for coastal waters that optimize the water-leaving radiance signal over many different wavelengths (Gould and Arnone, 1998), but these techniques require in situ measurements during the collection of the remote sensing data. New techniques under development by ONR Investigators (See C. Mobley, N00014-04-C-0218 and N00014-04-M-0108, and W. Bissett, N00014-01-1-0201 and N00014-04-1-0297) suggest that inversion techniques that use the entire spectra of the upwelling radiance field may offer the potential estimate bathymetry, IOPs and water clarity, and bottom type, simultaneously (Mobley et al., 2004).

Forecasting the optical properties would allow the estimation of IOPs over operational time horizons (5-10 days). In addition to water clarity estimates for NSW uses, these IOP estimates would also provide critical inputs for in-water optical sensor performance models such as laser line scanners used in MCM operations. This would allow for the efficient planning of NSW operations and MCM system deployments over an operational window. In addition, it would also facilitate the efficient allocation of environmental sampling resources such as AUVs during critical times of operational planning in both Naval operations and environmental studies, i.e., adaptive sampling. Such forecasting requires the coupling of a time-dependent ecological and optical model with a robust predictive physical model. Achieving a valid forecast of coastal IOPs would demonstrate the successful coupling of advanced predictive physical and ecological models, and would also demonstrate (at least to 1st order) that a fundamental quantitative understanding of the physical, chemical, biological, and optical processes operating in the marine environment had been achieved. Lastly, we hypothesize that predictions of in situ IOPs could be used by advanced inversion algorithms as a means of constraining their optimization equations. In addition, the remote sensing data would provide an ideal initialization and validation data stream with which to constrain both the physical and ecological simulations. Thus, it is clear that the future development of both optical remote sensing techniques and predictive models of IOPs would benefit by being coupled together.

This project is part of a larger effort to facilitate this development. It is a collaborative effort with many of the PIs in ONR's Hyperspectral Coastal Ocean Dynamics Experiment (HyCODE) and, in particular, we were funded as a Co-Principal Investigator, along with M Moline (California Polytechnic State University; N00014-99-1-0197), as part of a larger project led by O. Schofield (Rutgers University, Award N00014-99-1-0196). The report of this format will show the yearly progress, as well as summarize the major advancements to date.

WORK COMPLETED – FY 1999

The short-term prediction of the inherent and apparent optical properties requires accurate prediction of the physical, chemical, biological, and optical interactions of the oceanic environment. Such an undertaking is an imposing feat, and requires far more than a single investigator could hope to accomplish. However, this goal provides the background against which our efforts are measured. Working within a larger framework of experimentalists and physical numerical modelers, we are collecting and analyzing hyperspectral data, both in situ and from remote-sensing platforms, and modifying ecological code to develop the data assimilation techniques necessary for prognostic optical simulations.

This program is to focus on the data collected as part of the Coastal Predictive Skill Experiments (CPSE) each summer at the LEO-15, offshore of Tuckerton, NJ. The CPSE represented a multi-institution effort funded by ONR through the Hyperspectral Coupled Ocean Dynamic Experiment (HyCODE), the Coastal Ocean Modeling and Observation Program (COMOP), and the two awards from the National Ocean Partnership Program. Figure 1 shows a pseudo-RGB image of the LEO-15 site created from an AVIRIS in July of 1998.
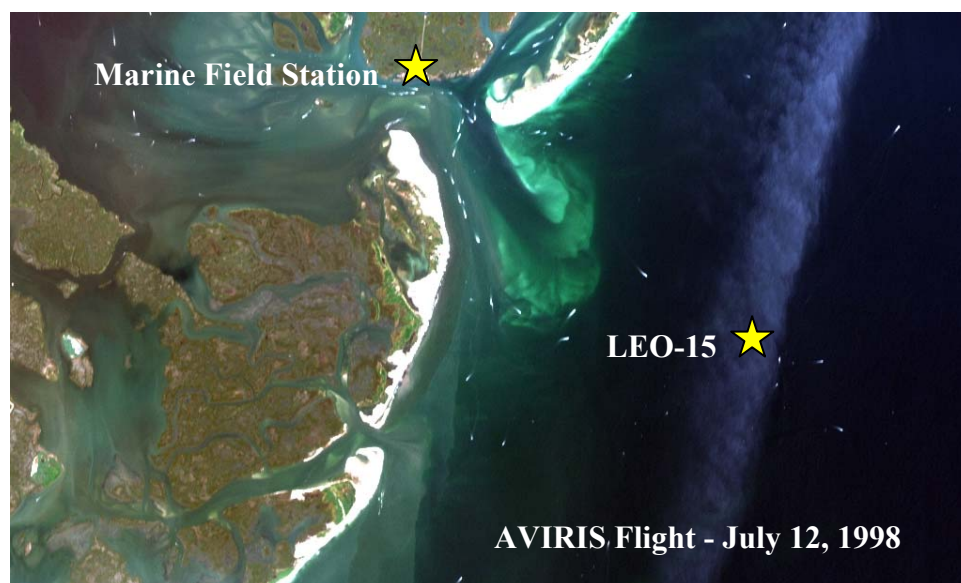

Figure 1. AVIRIS Pseudo-RGB Image from LEO-15 showing HyCODE Field site.

Addition hyperspectral data have been collected as part of the ONR COBOP field experiment at Lee Stocking Island (LSI), Bahamas. Our participation in the COBOP experiment focused on data

collection and inter-calibration of a new hyperspectral surface water buoy from Satlantic, Inc. (Satlantic H-TSRB), which is to be deployed at the LEO-15 site in July 2000.

Critical to the development of short-term optical forecasting simulations is an accurate initialization and validation data stream. Much of the work of this program was to focus on the collection of the optical data and its rendering into large scale maps of IOPs. A large fraction of this data stream was to be collected by either hyperspectral imaging spectrometers (mounted on aircraft or satellites) or autonomously mooring hyperspectral radiometers. Upon review of the hyperspectral AVIRIS data from LEO-15, the Ocean PHILLS data from LSI, and the upwelling radiance data from the H-TSRB (0.6 m depth), it became clear that any hyperspectral data assimilation technique would require some means to ground-truth the values of the water-leaving radiance, $L_w(\lambda)$, or remote-sensing reflectance, $R_{rs}(\lambda)$, being collected. Analysis of the image data suggested that there were major difficulties in validating the sea surface, water-leaving radiance values. These difficulties fell mainly into two divisions, instrument calibration and atmospheric correction. While these problems are beyond the scope of this research project, accurate hyperspectral data is critical to the success of our project. Thus, we tried to provide a means to use the H-TSRB to ground-truth the hyperspectral images, such that those working on instrument calibration and atmospheric correction issues will have accurate data to resolve their issues. We choose to address these issues from a modeling standpoint with the COBOP H-TSRB investigators.

Additionally, as part of the initialization and validation effort, we attempted to address some of the description of particle-specific optical properties with Dariusz Stramski (Scripps Institute of Oceanography), Oscar Schofield (Rutgers University) and Mark Moline (California Polytechnic State University). In particular, we wished to create a database of particle-specific optical properties as a function of phytoplankton species, nutrient state, light history, temperature, and cell size. These data will be used in EcoSim to produce temporally varying estimates of depth-dependent IOPs. In collaboration with Scott Glenn and Dale Haidvogel (Rutgers University), the completed coastal ocean EcoSim 2.0 will be coupled with the Rutgers University SCRUM model of the physical circulation of the New York Bight.

The FY 1999 work (9 months) was focused in two areas.

1)   Developing the methodology to create a database of particle-specific absorption, scattering, and scattering phase function for multiple groups of phytoplankton as a function of spectral light and nutrient history, temperature, and cell size.

2)   The collection of hyperspectral data with the H-TSRB, and modeling the changes in depth-dependent $E_d(\lambda)$ and $L_u(\lambda)$, and surface water $L_w(\lambda)$ and $R_{rs}(\lambda)$ as a function of bathymetry, pigment concentration, solar elevation, wind speed, and bottom type in an attempt to derive a simple relationship between the H-TSRB and the aircraft-collected hyperspectral images.

RESULTS – FY 1999

It is still early in the formulation of the optical database. While the framework is based on previous work (Stramski and Mobley, 1997), the data required to specify the changes in IOP for the various phytoplankton species is being compiled from many different investigators, and across decades of phytoplankton research. These data frequently do not contain the entire suite of particle specific optical properties (hyperspectral absorption, scattering, index of refraction, and scattering phase

function) that we would like to have, so new interpolation schemes will have to be developed to attempt to derive these data from limited data sets. In addition, new experiments are contemplated to collect the entire suite of specific optical properties over a range of light and nutrient conditions.

In attempting to develop a simple methodology to validate remotely collected $L_w(\lambda)$ with the H-TSRB, we were hearten by the relationship seen in Figure 1. The surface water reflectance ratio is defined as:

$$R(\lambda) = \frac{L_w(\lambda,0^+)/E_d(\lambda,0^+)}{L_u(\lambda,0^-)/E_d(\lambda,0^-)} \tag{1}$$

This ratio appears to be stable across the visible spectrum in an idealized, deep-water simulation. We thought that with minor modification we could apply this to the shallow water conditions seen around LEO-15 (Figure 1) and LSI. If this ratio is truly stable, and the values for $L_u(\lambda,0^-)$ could be estimated from $L_u(\lambda,0.6)$, then a simple methodology to ground-truth hyperspectral images could be developed. Thus, we define a ratio called, $R_{TSRB}(\lambda)$:

$$R_{TSRB}(\lambda) = \frac{L_w(\lambda,0^+)/E_d(\lambda,0^+)}{L_u(\lambda,0.6)/E_d(\lambda,0.6)} \tag{2}$$

Figure 3 shows the deep-water results assuming both a 2 m and 5 m slab of well-mixed water, overlying an infinitely deep water column. While there are some differences between the high chlorophyll a, low chlorophyll a, and actual LSI AC-9 data runs, the largest differences are confined to the region greater than 700 nm. As the veracity of aircraft hyperspectral data is marginal at these longer wavelengths, this did not appear to be a major roadblock in our efforts. From these runs it still appeared that the H-TSRB could provide simple, direct validation of the image data in collected in optically shallow waters.
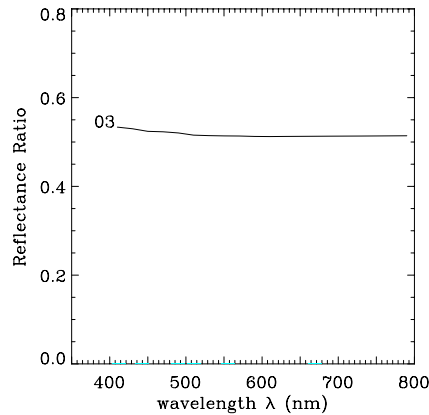

Figure 2. $0^+/0^-$ Reflectance Ratio. Hydrolight 4.02 calculation, Case 1 optical model, constant 0.05 chlorophyll a, 2 meters of water, infinite bottom, 45 degree sun angle, no clouds, 2 m/s wind.
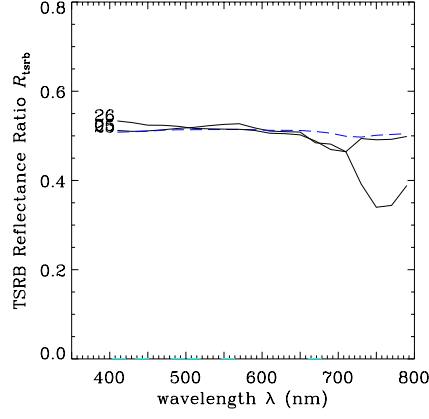
5

Figure 3(a). 2 meter infinite bottom calculations. Case 1 optical model IOPs with 0.05 and 10.0 chlorophyll a concentrations, as well as AC-9 IOPs from Rainbow garden with 0.05 chlorophyll a (for fluorescence).
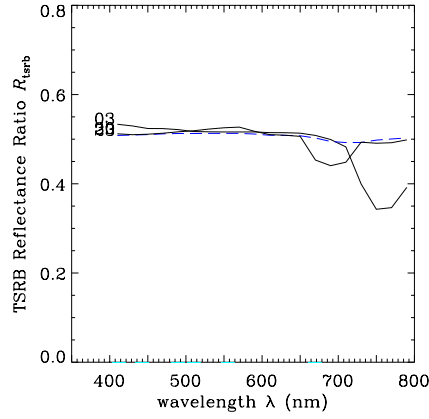

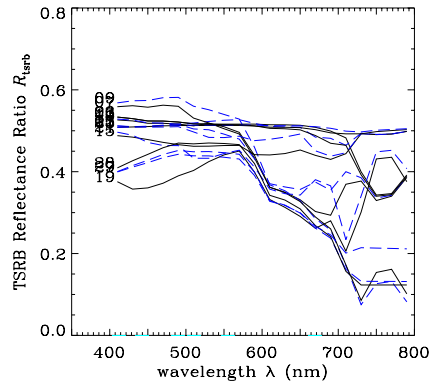*Figure 3(b). 5 meter infinite bottom calculations. Same parameter set as Figure 3(a).*

Figure 4. R_{TSRB} under varying depth, bottom types, and IOP conditions.

However, Figure 4 shows a subset of >60 Hydrolight 4.02 runs in shallow water conditions that were accomplished while trying to address this issue. As is evident, the shallow water $R_{TSRB}(\lambda)$ is anything but stable. In addition, there is very little pattern to the variation between the different runs (at least to a 0th or 1st order). These results suggest a simple relationship between surface water reflectance and $R_{TSRB}(\lambda)$ in optically shallow water may be difficult find, and usage of this data to directly ground-truth hyperspectral aircraft images may be tenuous.

Perhaps a better method of ground-truth would be to create a large database of Hydrolight solutions. Then, one could use look up-tables, neural networks, or optimization schemes to search this database to determine the best fit between the surface water AOPs, and depth-dependent IOPs. By developing a methodology of running multiple IOP scenarios through Hydrolight, including depth-dependent water-column IOPs, eventually a large data space could be created that would cover virtually all possible combinations. While time consuming up front, each run would only have to be accomplished once. Such a data set could then be given to the community as part of an algorithm that calculates bathymetry, bottom type, and depth-dependent IOPs simultaneous. These methods are currently being pursued by Kendall Carder (USF) and Curtiss Davis (NRL).

On the positive side, the deep-water solutions (Figure 3) show promise in providing a relationship between surface water reflectance and the reflectance measured by a tethered buoy. This may provide a means to ground-truth hyperspectral images over optically deep waters. We intend to explore the functionality of this relationship during the HyCODE LEO-15 field experiment in July 2000.

WORK COMPLETED – FY 2000

Objective 1
As part of this project, the Florida Environmental Research Institute (FERI) was given a Hyperspectral Tethered Spectral Radiometer Buoy (H-TSRB) built by Satlantic, Inc. Our goals include using this instrument to vicariously calibrate aircraft and remote sensing data to retrieve accurate water-leaving radiance measurements for algorithms development and model validation. This instrument was designed for the HyCODE program, and as such there are some validation/calibration issues on which we are still working. In a continuing effort, we deployed this instrument on a NASA Sensor Inter-comparison and Merger for Biological and Interdisciplinary Ocean Studies (SIMBIOS) funded cruise to the Northwest Passage of the Tongue Of The Ocean (TOTO), Bahamas with K. Carder of the University of South Florida (USF). The chief purpose of the experiment was to measure the apparent and inherent optical properties of the upper water column during overpasses of the NASA ocean color satellites, SeaWiFS and MODIS. We used this opportunity to further our experience with this instrument in a controlled, well-defined, environment.

Objective 2
We were initially to attempt a 1-dimensional simulation of the IOPs at LEO-15 on either side of an upwelling gyre, which was hypothesized to occur each summer at this location. This first series of numerical experiments was designed to familiarize the ecological and optical modelers with the LEO-15 site, and update the oceanic components of ecological code to those more relevant to coastal ocean dynamics. However, during the 1998 and 1999 field seasons (funded by ONR Coastal Ocean Modeling and Observation Program (COMOP) and the two National Ocean Partnership Program (NOPP) awards), the anticipated gyre did not form. Instead, strong coastal currents in excess of 100 cm s-1 frequently impacted the site. This meant that each day the water at the study site was replaced, rendering any attempt at a 1-dimensional model less than relevant to the measured IOP dynamics.

Thus, we decided to directly begin the 3-dimensional modeling effort. This required (and is still requiring) an extensive amount of code writing, recalibration of parameters, and incorporation of advective transport mechanisms. The lion share of this effort was completed, and was accomplished in collaboration with resources devoted to Award N00014-98-1-0844. The remainder was to be accomplished in November 2000, and a coupled EcoSim 2.0/ROMS model was to be available for the 2001 HyCODE field season.

Objective 3
The IOP and AOP equations of EcoSim 1.0 were designed for oligotrophic oceanic conditions. These equations have not been as useful in describing the optical properties of near-shore environments. In particular, the IOPs of the particulate material, both living and non-living, require a more complete mathematical description. The best approach for the living material would be to have the absorption, scattering, and phase function descriptions of individual phytoplankton groups, as well as the rates of change of these parameters as a function of light and nutrient history of the cells. However, this is time intensive laboratory work. While we are currently helping other investigators design the necessary experiments, our objectives require that we attempt to better approximate the IOPs with current information. The major addition to the living particulate IOPs is in the form of co-varying non-pigment absorption equations. Lastly, we have altered the specific-absorption of water from the previous EcoSim 1.0 description (Smith and Baker, 1981) to one considered more correct by the ocean optics community(Pope, 1993; Pope and Fry, 1997). This impacted a number of equations and parameters, which had to be modified for the lower specific-absorption in the blue.

RESULTS – FY 2000

H-TSRB
In accordance with the SIMBIOS project guidelines for instrument calibration, the H-TSRB was returned to Satlantic for radiometric calibration immediately prior to TOTO cruise. As a check on the accuracy of the calibration, a comparison was made of the downwelling irradiance modeled by RADTRAN (Gregg and Carder, 1990) and that generated by a handheld spectral radiometer, Spectrix #300, and a Spectralon reflectance target. The Spectrix was radiometrically calibrated on April 11-14, 2000 by two methods: one based on tungsten lamp with spherical integrating sphere and the other based on direct and global solar irradiance (Biggar, 1998). In addition, the bi-directional reflectance function of the Spectralon target was calibrated with respect to a NIST-supplied reflectance target. Of all the samples on TOTO where coincident samples were collected, only four were deemed sufficiently cloud-free and calm enough to avoid perturbations in the measurements. The comparison of measured and modeled downwelling irradiance, $E_d(\lambda)$, during the TOTO cruise is illustrated in Figure 5.

In general, the H-TSRB appears to give significantly higher readings throughout the spectrum in relation to the modeled (rad) and the Spectrix (spx) measurements. The model and Spectrix irradiances are in good agreement except for Station 1, where data were collected at a higher solar zenith angle. Further work was started to determine the reasons for the differences, but it was clear that a problem exists that must be rectified prior to accepting the data from the H-TSRB as appropriate for vicarious calibration for aircraft remote sensing. It was unclear whether the fault lay with the instrument itself, or our operation of the instrument. We explored potential faults with our methodology prior to raising the issue with Satlantic, Inc.
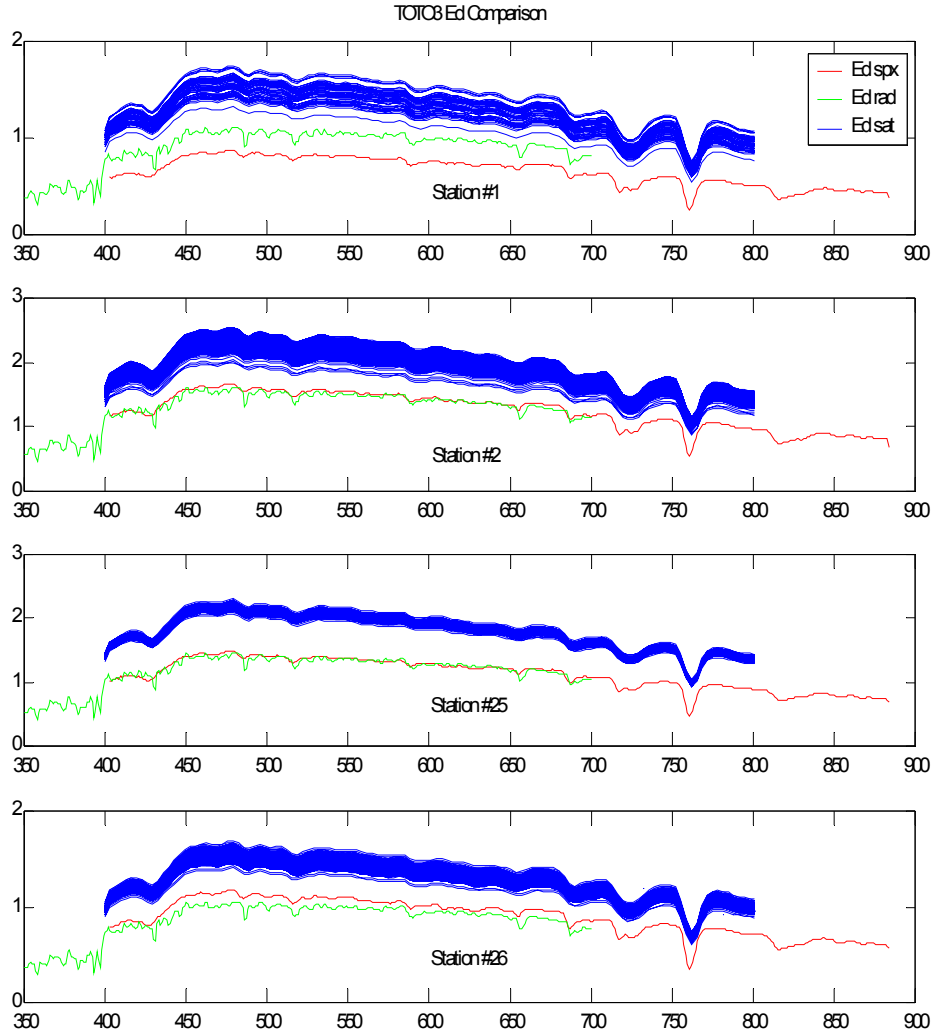
Figure 5. Comparison of downwelling irradiance (W/m²/nm) as measured by the Spectrix/Spectralon (spx) and the Satlantic H-TSRB (sat), and modeled (rad) for four cloud-free, relatively calm stations on TOTO.

EcoSim 2.0

It was determined after consultation with ROMS developers that the best way to approach the coupling of the current 1-D code was to develop an ecological/optical model that could read in diagnostically the advective fluxes simulated from the 3-D model. The increase in the dimensionality and addition of advective transport coding to the EcoSim 2.0 was completed during this time period. (In addition, we also increased the number of phytoplankton functional groups and nutrient pools under other ONR funding). We tested this advective transport model in a 2-dimensional series of numerical experiments on the West Florida Shelf (WFS). Figure 6 is an example of the cross-shelf particulate and dissolved IOPs for the month of November 1998 in response to a Loop Current intrusion onto the shelf. It was clear from these results that the advective fluxes dominated the time-dependent optical processes in determining the state of the water column IOPs. In addition, these results demonstrated the importance

of boundary conditions to forecasting IOPs. In this case, the deep water boundary conditions, coupled with the advective flow through the boundary, brought nutrient rich water into the euphotic zone, which resulted in increase phytoplankton biomass and increased total absorption.
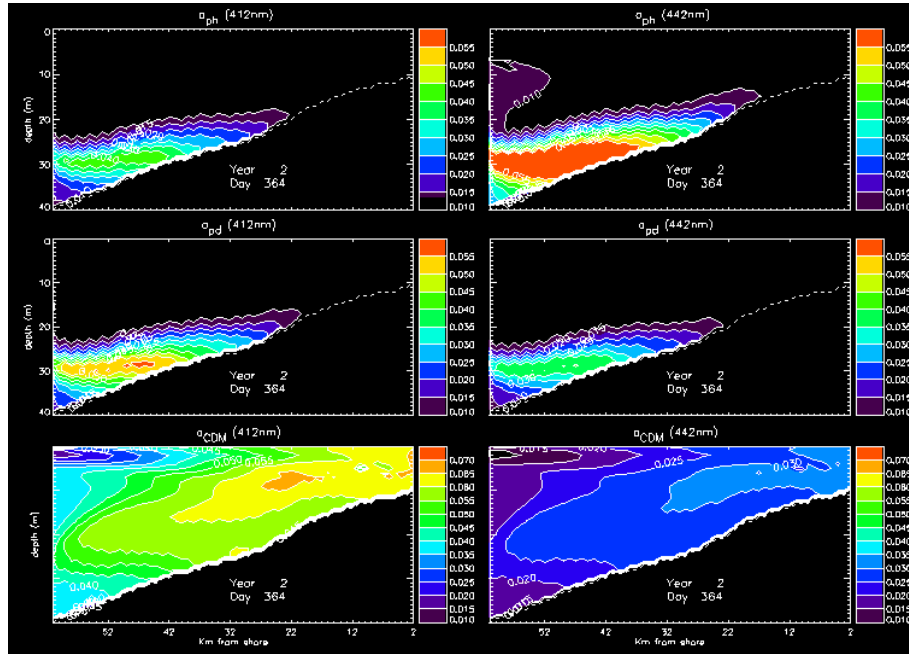

Figure 6. Particulate and dissolved absorption at 412 and 442 nm. Top panels) total pigmented absorption, $a_{ph}(412)$ and $a_{ph}(442)$; middle panels) total non-pigmented absorption, $a_{pd}(412)$ and $a_{pd}(442)$; bottom panels) total CDOM and detrital absorption, $a_{CDM}(412)$ and $a_{CDM}(442)$.

WORK COMPLETED – FY 2001

LEO-15 Field Deployment
FY 2001 was the major LEO-15 HyCODE field deployment, including our participation with in situ instrumentation, as well as being responsible for the deployment of the NRL PHILLS-2 hyperspectral imager (see W. Bissett, N00014-00-1-0514). We continued to develop the H-TSRB data stream as a means to validate and atmospherically-correct our hyperspectral imager data, as well as obtain input data needed for the forecasting of the inherent optical properties. This included comparing the H-TSRB data from the 2001 experiment and comparing it to the RADTRAN simulation data (Gregg and Carder, 1990) for the same time period. This RADTRAN data is used as input for the EcoSim/ROMS simulation.

ROMS/Ecosim 2.0
The ROMS developers felt that the current method of off-line physical simulations were too difficult to support and required addition runtime to complete, so this year's major modeling focus was to complete the re-coding of EcoSim 2.0 so that it would be compatible with an on-line version ROMS physical circulation code (http://marine.rutgers.edu/po/models/roms.html). In fact, we attempted to complete the coupling of the two codes for on-line simulations prior to the HyCODE July 2001 field campaign. (On-line simulations refer to both codes running simultaneously rather than the physical output used in an off-line run of the ecological/optical forecast). This was a much more significant endeavor than the recoding of EcoSim 1.0 to handle 3-dimensional advective flow fields from the

ROMS code (see last year's progress report), in that we had to significantly reduce the code space, alter the flow of the ecological code, and reduce our error checking procedures, while maintaining the integrity of the calculations, in order to run with the highly compact, parallel version of ROMS. It was felt by the ROMS developers that this coupling of in-line codes would facilitate a more rapid demonstration of the predictive capabilities of the EcoSim/ROMS optical forecast system, thus increasing the probability of achieving the overall HyCODE goals.

RESULTS – FY 2001

Field Data
Figure 7 shows the comparison between RADTRAN and H-TSRB on July 30, 2001. There appears to be a reasonable agreement between the simulated downwelling irradiance and the measured downwelling irradiance. However, there were some differences in the blue that require some further analysis. In addition, it also appeared that there are some extreme dips in the RADTRAN data that are not seen in the H-TSRB data. It was thought that these differences will probably not have much impact on the ecological simulation or the IOP prediction; however, it may have a direct impact on predictions of L_w and the atmospheric correction of the PHILLS-2 data.
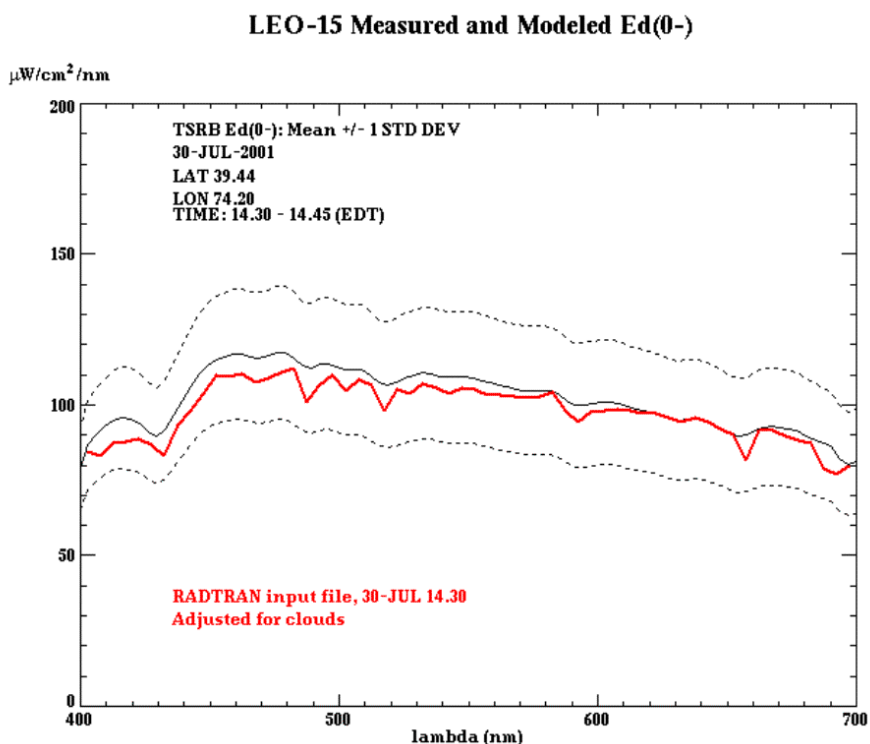
Figure 7. Modeled and Measured Downwelling Irradiance at the Sea Surface. Modeled data from RADTRAN, measured data from H-TSRB on July 30, 2001.

ROMS/EcoSim
We completed the re-coding as well as demonstrated the parallel version of EcoSim/ROMS. Unfortunately, while the coding was completed prior to the field experiment, debugging was not. While at Rutgers Marine Field Station, we were able to complete the debugging to the coupled code,

but not before the end of the experiment. Figure 8 shows the test case example of a chlorophyll a transect through an idealized 5 by 80 gridded basin with an upwelling favorable eastern edge and a downwelling favorable western edge. For this test case, EcoSim was run with 60 wavelength bands, 4 phytoplankton functional groups of phytoplankton, 7 phytoplankton pigments groups, 6 nutrient pools, 2 DOM pools, 2 CDOM pools, and 2 detritus pools, and included the IOP descriptions of the optical constituents.
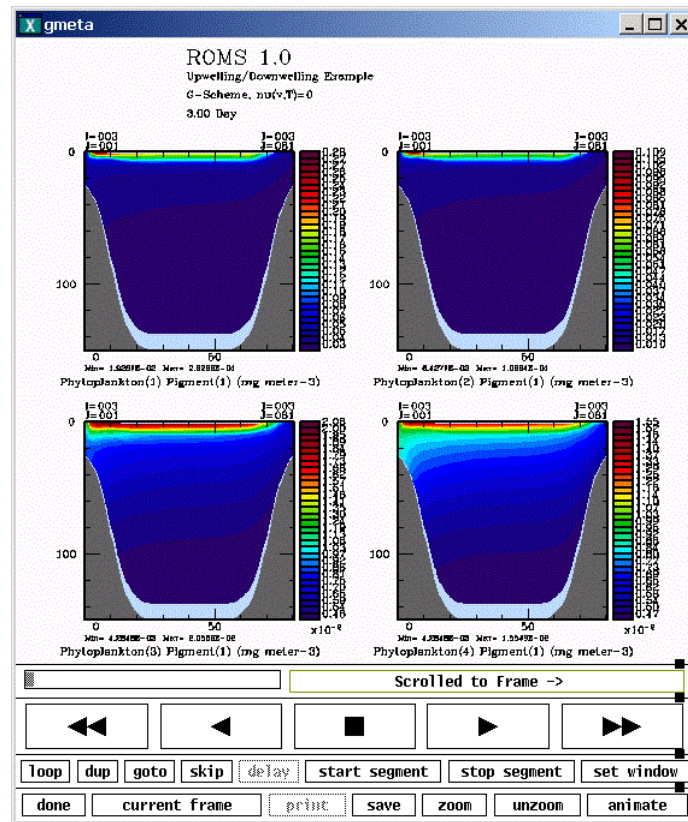
Figure 8. Example of EcoSim/ROMS output from 3-dimensional idealized basin. This simulation used idealized upwelling and downwelling favorable winds on each side of the basin. Contours are chlorophyll a for each functional group.

WORK COMPLETED – FY 2002

ROMS/EcoSim

One of the goals of ONR's Environmental Optics Hyperspectral Coastal Ocean Dynamics Experiment (HyCODE) program was to develop the forecasting ability to predict the depth-dependent optical constituents, and their impact on water-leaving radiance and water-column visibility. The satisfaction of this optical goal requires the ability to forecast the physical oceanographic environmental, such that the distribution and time-dependent change of the optical constituents can be adequately represented in a 4-dimensional framework. In pursuit of these nowcast/forecast objectives, HyCODE sought to build partnerships with ongoing research programs focused on the short-term prediction of the coastal circulation. Thus, the development an ecological and optical forecasting model was embedded into the Coastal Predictive Skill Experiments being conducted off of the coast of New Jersey during the summer of 2001. The modeling system described here is an implementation of the coupled ROMS

(Regional Ocean Modeling System)/EcoSim (Ecological Simulator) model developed for ONR's HyCODE and Coastal Ocean Modeling and Observation Program (COMOP).

ROMS is a free-surface, hydrostatic, primitive equation model initially based on the s-coordinate Rutgers University Model (SCRUM) described by (Song and Haidvogel, 1994). ROMS was rewritten by the UCLA and Rutgers ocean modeling groups to improve its numerics and efficiency in single and multi-threaded computer architectures. New features include high-order advection schemes; accurate pressure gradient algorithms; several subgrid-scale parameterizations; atmospheric, oceanic, and benthic boundary layers; radiation boundary conditions; and data assimilation.

EcoSim is an upper ocean ecological model initially based on the differential elemental cycling model used to describe the impacts of phytoplankton ecology on oceanic carbon cycling (Bissett et al., 1999a; Bissett et al., 1999b). This initial work focused on inorganic and organic carbon cycling, and found that the dynamics of carbon cycling in the upper ocean depended on speciation of the phytoplankton community. This was not a new concept, but they demonstrated the numerical extrapolation of some key ecological hypotheses relating to carbon cycling. The success at the simulated interactions between spectral light, nutrients, and phytoplankton speciation provided justification to expand the simulated phytoplankton diversity and elemental representation, as well as to incorporate the model into the three dimensional ROMS nowcast/forecast system of the Middle Atlantic Bight.

EcoSim incorporates the non-stoichiometric nutrient dynamics of the phytoplankton population by allowing luxury uptake and non-balance nutrient growth. In addition, photosynthetic light harvesting is pigment specific and depends on growth rate, cellular nutrient content, and light history. DOM cycling includes 2 forms (labile and recalcitrant) of DOC, DON, and DOP, as well as explicit spectral description of 2 forms of CDOM. Differential regeneration of the nutrients into organic and inorganic element forms completes the non-stoichometric cycling of macro- and micro-nutrients. The current version of ROM/EcoSim for the Middle Atlantic Bight contain equations for 7 functional groups of phytoplankton (2 diatoms, 2 dinoflagellates, 2 prochlorococcus, and 1 synechococcus), but is typically run with only 4 (2 diatoms, 1 dinoflagellate, 1 synechococcus) to optimize runtime efficiency. The total numbers of independent state variables for the simulations during the ONR COMOP/HyCODE program are 62, as the description of each phytoplankton contains state equations for functional group carbon, nitrogen, silica, phosphorus, and iron, as well as state equations for each individual pigment within each functional group. Since the model tracks each state variable through mass conservative calculations, all are available for validation of the ecological forecasts. In other words, the model can be validated by measurements of DIC, NH4, NO3, PO4, SiO4, DOC, DON, DOP, POC, PON, POP, POSi, POFe, TOC, TON, TOP, TOSi, TOFe, phytoplankton counts, total chlorophyll (see Figure ROMS/EcoSim), HPLC pigments, as well as the optical measurements of spectral absorption, scattering and water-leaving radiance. It is this explicit coupling of spectral optics to ecology, in addition to the non-stoichiometric nutrient dynamics, that makes this approach unique.

The shared memory parallel version (using OpenMP) of the ROMS/EcoSim code that we used to produce forecasts on the New Jersey coast for ONR's COMOP/HyCODE program (Arango et al., 2002) in July 2001 required 25 hours of wall clock time to process a 31 day simulation of a 100 x 240 (horizontal) x 25 (vertical) grid when executing on 16 (out of 256) processors of the NRL Origin3800 supercomputer (neo.cmf.nrl.navy.mil). The ecological and optical state variables were initialized from an analytical relationship between the state variable and temperature and salinity on July 11, 2001, and the simulation was run until August 8, 2001.
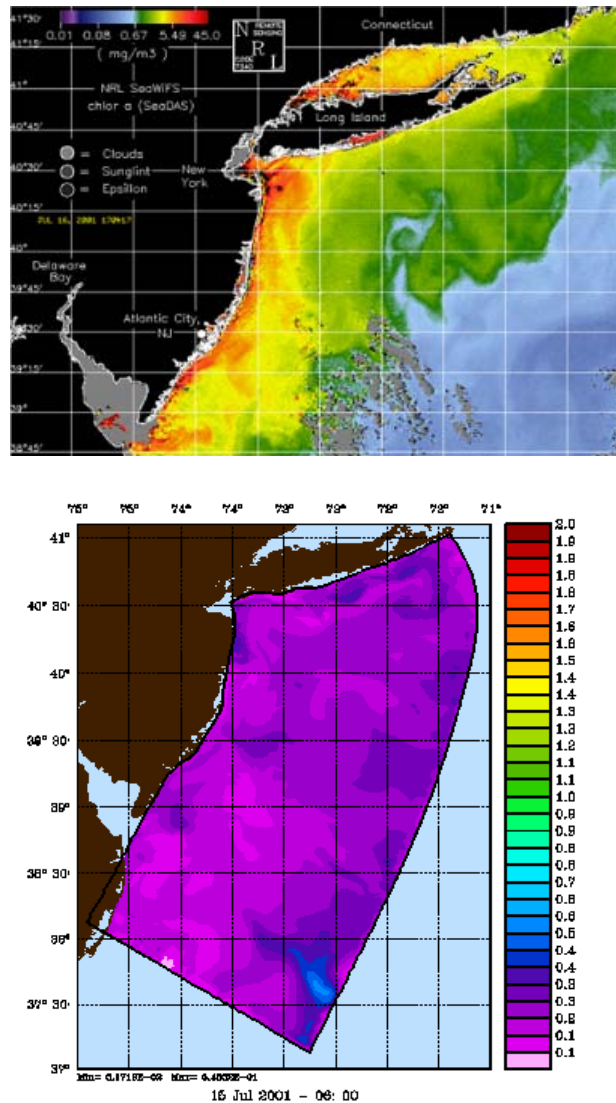
RESULTS – FY 2002

Figure 9. SeaWiFS Chlorophyll a estimate for July 15, 2001 (created by NRL-Stennis, Top), and Simulated Surface Chlorophyll a from ROMS/EcoSim (Bottom). The initialization value of the model total phytoplankton biomass was very low, rendering very low chlorophyll estimates relative to the satellite data.

The preliminary results from the coupled modeling are encouraging; however, they highlight the difficulties that will be faced in developing a prognostic simulation of IOPs. One of the major difficulties in these short term numerical experiments is the initialization of water mass constituents and numerical history of water mass properties. The initialization of the model is based on a historical analysis of the relationship between temperature and salinity and the state variables of the model. The assumption is that the system will rapidly respond to any discontinuities in the initial conditions as long as the forcing functions are accurate. However, if the forcing functions are in error, or the temperature and salinity values themselves are in error, these will have downstream consequences for the ecological and optical solutions. Figure 9 shows the estimated chlorophyll a field from SeaWiFS and the simulated total surface chlorophyll. Clearly, the simulated fields (Figure 9, Bottom) are much

lower than those of satellite estimates (Figure 9, Top). This is to be expected as the initialized fields were very low, but the beginnings are field structure is beginning to become evident. By August 8th (Figure 10) biomass as represented by simulated chlorophyll begins to show much greater accumulation as well as some coastal structures associated with upwelling features near the apex region of the NJB.
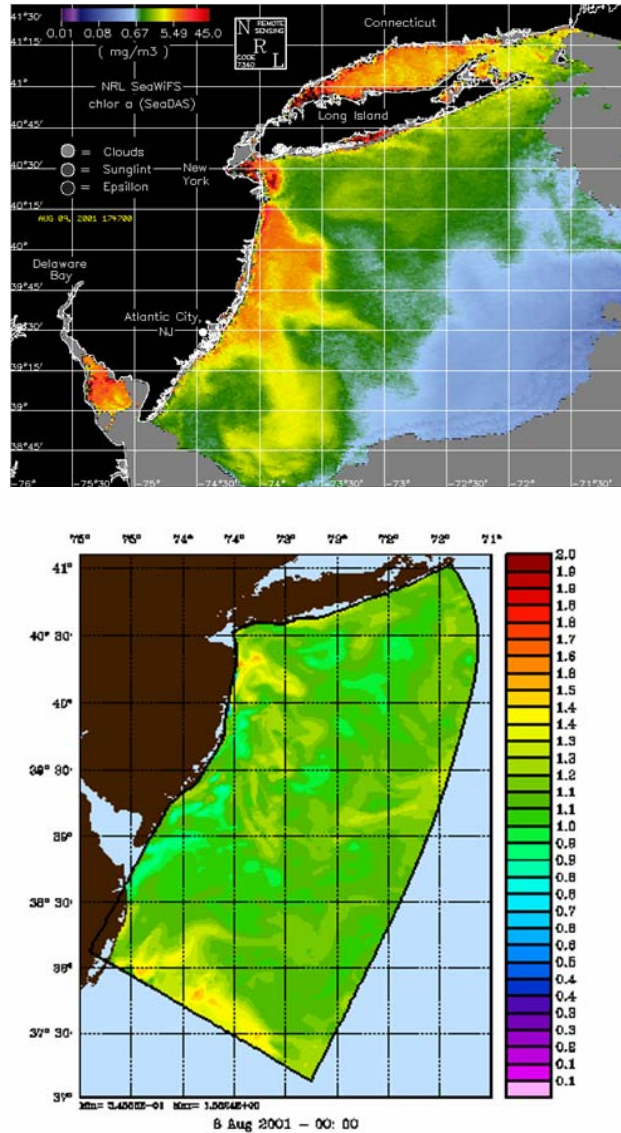
Figure 10. SeaWiFS Chlorophyll a estimate for July 15, 2001 (created by NRL-Stennis, Top), and Simulated Surface Chlorophyll a from ROMS/EcoSim (Bottom). The simulated values begin to approach the average values for the domain after a couple of weeks of simulated time.

There are some spatial discrepancies, particularly around the LEO site that are related to the history of the water masses. Figure 11 shows the SST from a morning pass of AVHRR and the simulated temperature field on the July 15th. There are two simulated "hot" water features that are not evident in the AVHRR fields. These features are advected towards the shore by the 21st. While discrepancies of the simulated temperatures are reduced as time progresses, the simulated history of the water mass "remembers" the higher temperatures, as the growth and grazing processes are significantly different

for the warmer waters. In this case, there is approximately a 50% increase in the growth and loss processes in the "hot" water, than would have been estimated from the actual data. The bigger impact appears to be on the loss processes as the nutrient fields are higher in the hot water mass, in spite of having been initialized at similar levels. These higher loss processes in this water mass reduce the biomass to levels that are unable to completely utilize the nutrient stocks, as well as reducing the total load of IOPs in the water column. The advection of these water mass onto the shore alters the expected IOPs (not shown) as these are a function of the biomass growth, loss, and accumulation processes.
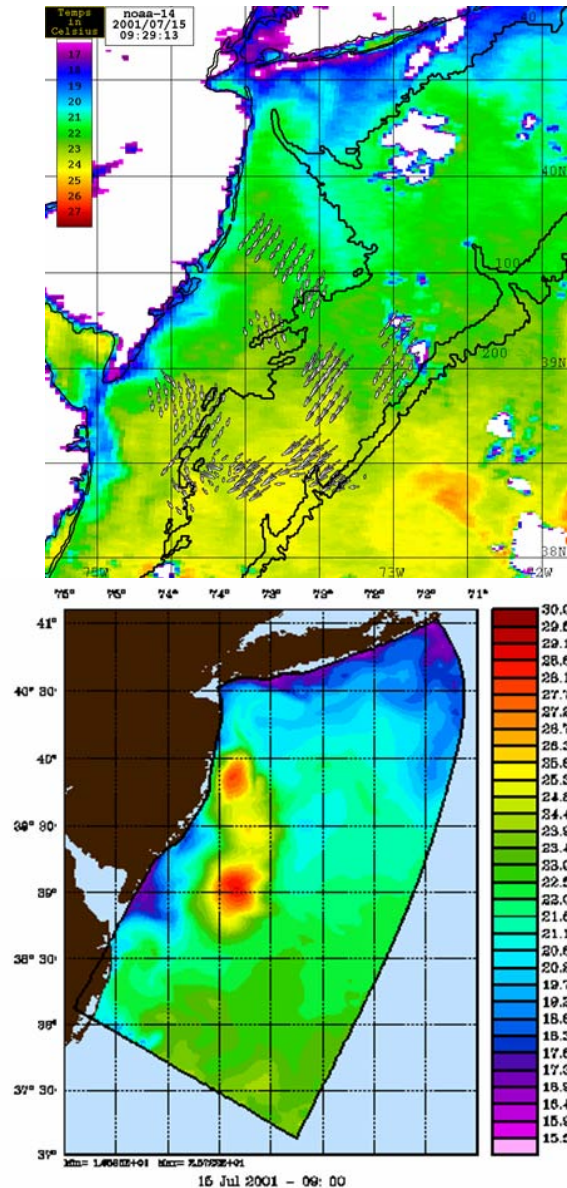
Figure 11. AVHRR SST (top) and simulated SST (bottom) on July 15, 2001. The "hot" spots in the simulated SST are a result of a poor assimilation scheme, and are not real. These caused significant errors in the ecological and optical results.

The hot water features appear to be artifacts of the data assimilation scheme used for temperature and salinity (Arango per. comm.). The assimilation scheme uses and interpolates field data into a three

dimensional grid, and then extrapolates the data across the domain of the model. In this case, it appears that the extrapolation of interpolated field data created water mass properties, outside of the collection domain, that were unrealistic. While these values were not evident in the LEO domain during the course of the COMOP experiment, there inclusion into the larger domain impacted the ecological and optical history of the water masses that were advected into the LEO domain.

Addendum to the FY 2002 ROMS/EcoSim Efforts
It became evident upon closer inspection of the physical model that there were many things wrong with the physical code besides the assimilation scheme. There were code bugs (e.g. tides that were 180 degrees out of phase) and logic errors (e.g. bathymetry that was in error beyond 100 m), that rendered this physical circulation simulation less that useful. The reason it worked so well inside the LEO-15 domain was that the COMOP and HyCODE field teams provided so much hydrographic data that the hydrodynamics model was over-constrained in the assimilation process, and forced to match the measurements. Outside of the LEO-15 domain, where there was little or data to assimilate, the solutions appeared less than robust. This version (ROMS v1.8) was the third version of ROMS for which we had rewritten the EcoSim subroutines. The errors in the ROMS v1.8 led to a complete overhaul of the code to version 2.0.

WORK COMPLETED – FY 2003

Field Data
The 2001 LE0-15 field experiment (July 21-August 3, 2001) provided a uniquely coordinated opportunity with a variety of remote sensing imagery collected simultaneous to a small fleet of vessels, moorings, and a buoy with optical ground truth measurements. Imagery was collected by satellite (SEAWIFS), high altitude aircraft (AVIRIS @ 20km), medium altitude aircraft (PHILLS2 @10km), and low altitude aircraft (PHILLS1@ 300m). To further close the loop on atmospheric correction, the Florida Environmental Research Institute along with the University of South Florida's Ocean Optics Laboratory deployed automated and handheld sun photometers along with a meteorological station. From these instruments, aerosol optical depths, downwelling irradiance, ozone, air temperature, barometric pressure, and relative humidity were monitored during the over flights at the Rutgers University Marine Field Station (RUMFS near Tuckerton, New Jersey 39.508°N, 74.323°W). The data from these sensors was analyzed and prepared for publication, as well as for use in the atmospheric correction of both satellite and aircraft imagery.

ROMS/EcoSim
Following the discovery of errors in the data-assimilative ROMS physical circulation simulations at the end of FY 2002, we focused on running the simulation in a non-assimilative mode in order to test the robustness of the EcoSim/ROMS coupling. This allowed us to study the ecological response functions when driven by 3-D physical dynamics. This initial 3-D study led to some general ecological and IOP simulation successes; however, additional errors in the physical circulation model, (which were deemed too extensive to fix in the 1.8 version of ROMS) were found and these required fixing before additional ecological/optical studies could be completed. The physical modeling group has chosen to correct these errors with the soon to be release ROMS 2.0 version in order to generate physical simulations for the 2001 LEO field season. The 2.0 version of ROMS was developed for distributed parallel computing and nested model development (e.g. the high resolution LEO domain nested into the lower resolution North Atlantic domain). This required a significant amount of recoding of the EcoSim modules.

RESULTS – FY 2003

Atmospheric Measurements
During the LEO 2001 experiment, there were two days suitable for the generation of Langley plots (instrument voltage versus airmass), July 21st and 27th. Aerosol loading on all other days (July 31st, August 1st, and 2nd) proved to be too variable or had systematic increases that skewed regression despite being visually cloud-free. The intercepts from the 21st and 27th were then used to calculate the total and aerosol optical depths as well as Angstrom exponents summarized in Figures 12.
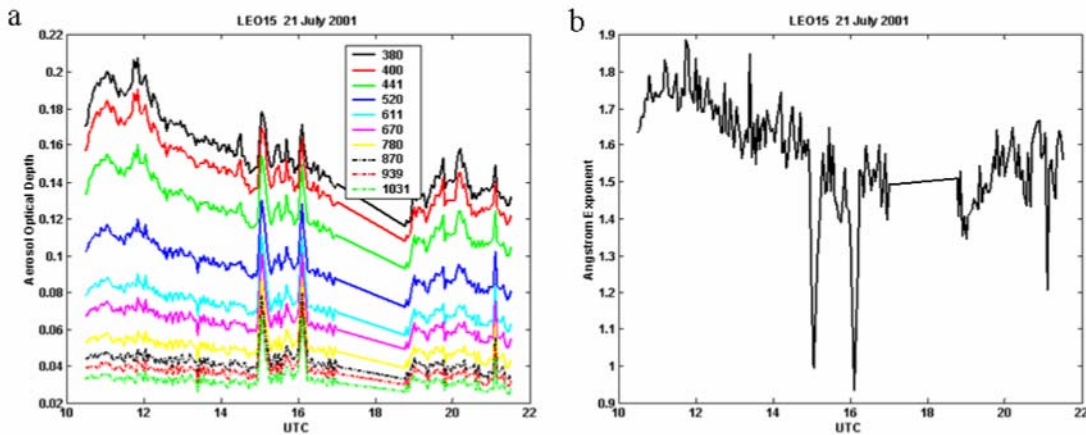

Figure 12. Aerosol Optical Depth (a) and Angstrom Exponent (b) during the July 2001 HyCODE LEO-15 experiment. July 21st and July 27th (not shown) had the most consistent airmasses during the experiment. Aerosol optical depth averaged approximately 0.035 for 1031 nm, increasing to approximately 0.16 for 380 nm. The angstrom exponent averaged approximately 1.6.

There were two distinct aerosol characteristics at LEO in response to frontal passages. Before the July 26th storm, the typical conditions were for aerosol optical depth, τ_a, on the order of 0.1-0.2 and an angstrom exponent, α, of 1.5-1.8. Immediately following the storm on the morning of July 27th, τ_a dropped to exceptionally low values of 0.07 -0.1 with α of 1.2-1.3. These were consistent throughout the day but are masked in the Automated Solar Radiometer (ASR) products by jet contrails. The larger storm event on July 29-30th produced a similarly clear atmosphere on July 31st. However, it rapidly degraded during the early morning hours. The τ_a climbed steadily throughout the next 60 hours from the lowest to highest values for the experiment, 0.07 – 0.50, and the α increased from 1 to 2, indicative of small particles typical of urban/continental aerosol models.

The first check on the ASR products was a comparison to those independently derived from other sensors on site and those derived from SEAWIFS processing. In addition to the ASR, two Microtops (one with ozone channels and the other with SEAWIFS channels) were deployed at various locations during the experiment. Two images from SEAWIFS were collected during the field experiment. Since the SEAWIFS overpass occurs close to local noon, the 7/27 image was collected after the contrails had dissipated and confirms the low aerosol concentration for the day. The 7/31 image shows that not only did the aerosol concentration increase with time, but also varied spatially.

Table 1: Comparison of Atmospheric and Aerosol Parameters. µt – Microtops handheld sun photometer, wv – water vapor (cm^{-1}), O3 – ozone (Dobson units)

	7/27/2001			7/31/2001		
	am	noon	pm	am	noon	pm
ASR τa550	0.05*	0.05			0.15	0.17
µNRL τa550			0.08-0.17	0.12-0.15		
SeaWIFS τa555		0.05-0.3			0.05-0.3	
ASR α550	1.4	1.5	1.6	1.4	1.3	1.5
SeaWIFS α555		0.2-1.4			0.2-1.4	
µUSF wv	0.7		0.6	1.3		1.6
µNRL wv			0.8-1.1	1.8-1.9		
SeaWIFS wv		1.2-1.4			1.8-2.6	
µUSF O3	324		330	324		309
TOMS O3		330			331	
*prior to contrail formation						
**broad distribution of values (0.02-1.5)						

The second is often called vicarious calibration. It entails selection of atmospheric correction parameters such as aerosol/ozone/water vapor to make the remote spectra match a known or measured ground target reflectance. Most of the airborne HSI at LEO was atmospherically corrected using *Tafkaa* (Montes et al., 2001), a tabularized version of the ATREM atmospheric model (Gao and Davis, 1997; Gao et al., 2000). At two sites on 7/31, the surface reflectance was measured during the over flights by two different, well-calibrated radiometers, one a Satlantic TSRB and the other an Analytical Spectral Devices FieldspecFR. Thousands of *Tafkaa* runs were conducted, optimizing the parameters until the atmospherically-corrected AVIRIS and PHILLS2 spectra best matched the reflectance spectra measured on the water. The aerosol optical depths are shown in Table 2.

Table 2: Optimized Atmospheric Parameters for 7/31

Imager-Target	τa550	aerosol model	ozone dobson	wind speed m/s	water vapor cm	relative humdity %
PHILLS2-TSRB	0.166	urban	340	2	0.525	70
AVIRIS-TSRB	0.108	urban	340	2	0.500	50
AVIRIS-ASD Rrs	0.137	urban	340	2	0.500	50
AVIRIS-ASD raw	0.064	urban	340	2	0.500	50

To demonstrate the importance of the aerosol to the atmospheric correction, a series of MODTRAN4 radiance calculations were performed using parameters appropriate for the 7/31/2001 am flight window and using the default spectral albedo for ocean. The aerosol contribution was varied from $\tau_a(550) = 0.5$ to 2.0 (or roughly a visibility range of 3 to 13 km). Figure 13 shows how the radiance at a 10 km height sensor is related to the surface reflected radiance. The large differences shown in the NIR is chief source of error in the atmospheric correction and the reason for deployment of sun photometers and the optimization schemes shown here.
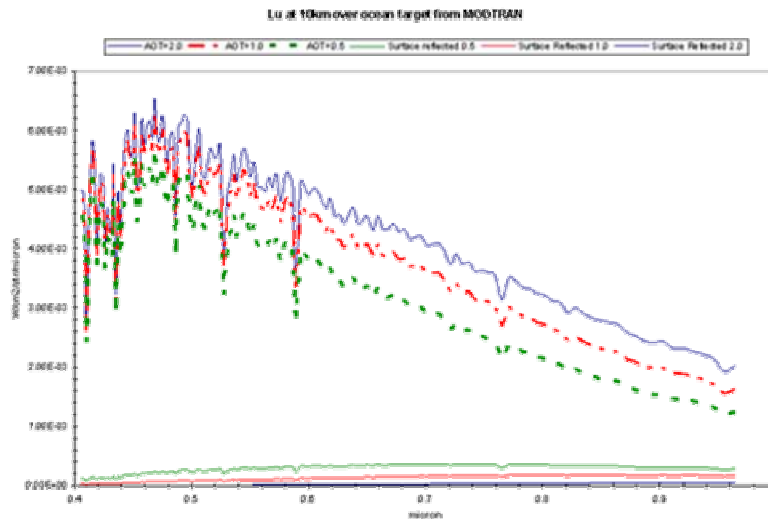
Figure 12. Upwelling radiance at 10 km altitude (upper three curves) for three different τa550 and atmospheric parameters for LEO15 on 7/31/2001 as modeled by MODTRAN4. Lower three curves are the radiance reflected from the default ocean surface in the model.

EcoSim/ROMS

There were a number of corrections to the physical code following the results of the previous simulation analysis, in part driven by errors in the assimilation scheme. The results shown here have been generated without the data assimilation scheme. This allows us to highlight the results of the coupled physical/ecological simulation without the errors in the assimilation scheme. Further physical errors are to be corrected in the ROMS/TOMS 2.0 release. The results shown are from the ROMS 1.8 release generated for the HyCODE 2001 field season and focus on August 2, 2001 (Figure 13 and 14). Figure 13 shows the surface plots around the LEO-15 sampling grid, and Figure 14 are from the N1 sampling line (as seen in the AVHRR and SeaWiFS images in Figure 13).

The ecological interactions between the phytoplankton groups yield differences between the accumulation of pigments and carbon biomass. The differences result primarily because of the differences in the carbon to chlorophyll ratios of each functional group. The total chlorophyll a associated with diatoms, cyanobacteria, and dinoflagellates are similar to that estimated by HPLC analysis, and most of the chlorophyll split between diatoms and cyanobacteria. Carbon biomass, however, is weighted between the functional groups differently, with cyanobacteria dominating the total carbon biomass. This has significant implication for remote sensing algorithms and prediction of water-leaving radiance. Absorption is most closely associated with total pigment concentration; however, scattering is more of a function of species and total carbon biomass (Stramski et al., 1999). Algorithms designed to detect types of phytoplankton, i.e., Harmful Algal Blooms, may have to resolve the difference between absorption and scattering at the species level. Once the physical issues are resolved in ROMS, the IOPs from this simulation will be used to drive predictions of water-leaving radiance using Ecolight (See Bissett ONR Progress Report, N00014-01-1-0456, and Mobley ONR Progress Report, N00014-00D01-61-0002). These will be directly compared to remote sensing upwelling irradiance measurements collected by PHILLS1, PHILLS2, AVIRIS, SeaWiFS, and MODIS sensors.

Large Diatom Carbon
μmol liter⁻¹

Small Diatom Carbon
μmol liter⁻¹

Dinoflagellate Carbon
μmol liter⁻¹

Cyanobacteria Carbon
μmol liter⁻¹

(note scale shift)

Surface Temperature
degrees

AVHRR SST
degrees

SeaWiFS Chl a
μgrams liter⁻¹

Total Chl a
μgrams liter⁻¹

Large Diatom Chl a
μgrams liter⁻¹

Small Diatom Chl a
μgrams liter⁻¹

Dinoflagellate Chl a
μgrams liter⁻¹
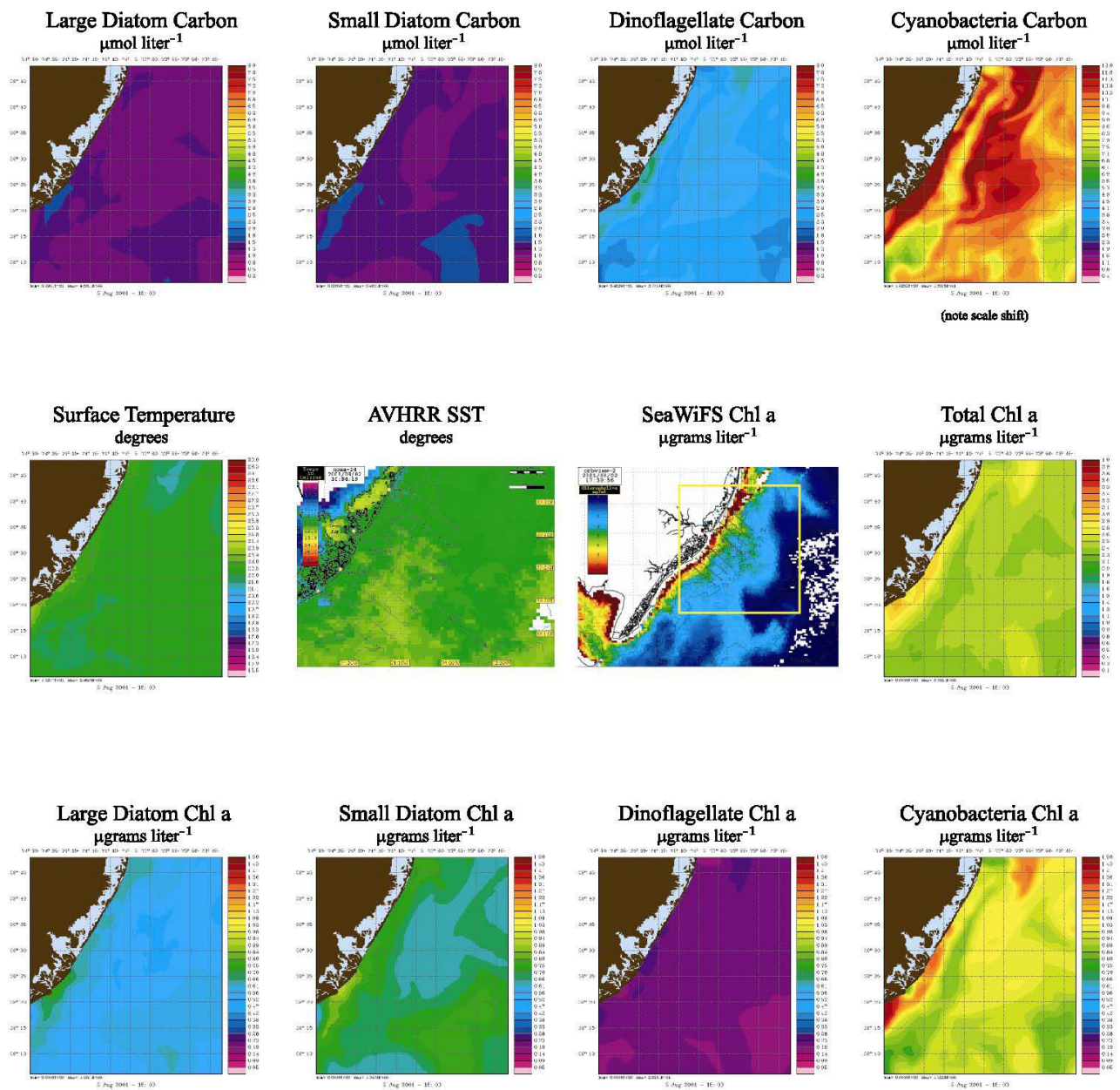
Cyanobacteria Chl a
μgrams liter⁻¹

Figure 13: Surface distribution of simulated carbon biomass per functional group (top row); simulated SST, AVHRR SST, SeaWiFS Total Chlorophyll, and simulated Total Chlorophyll (middle row); and simulated chlorophyll a per functional group (bottom row) at the LEO 15 field site August 2ⁿᵈ during HyCODE 2001 experiment.
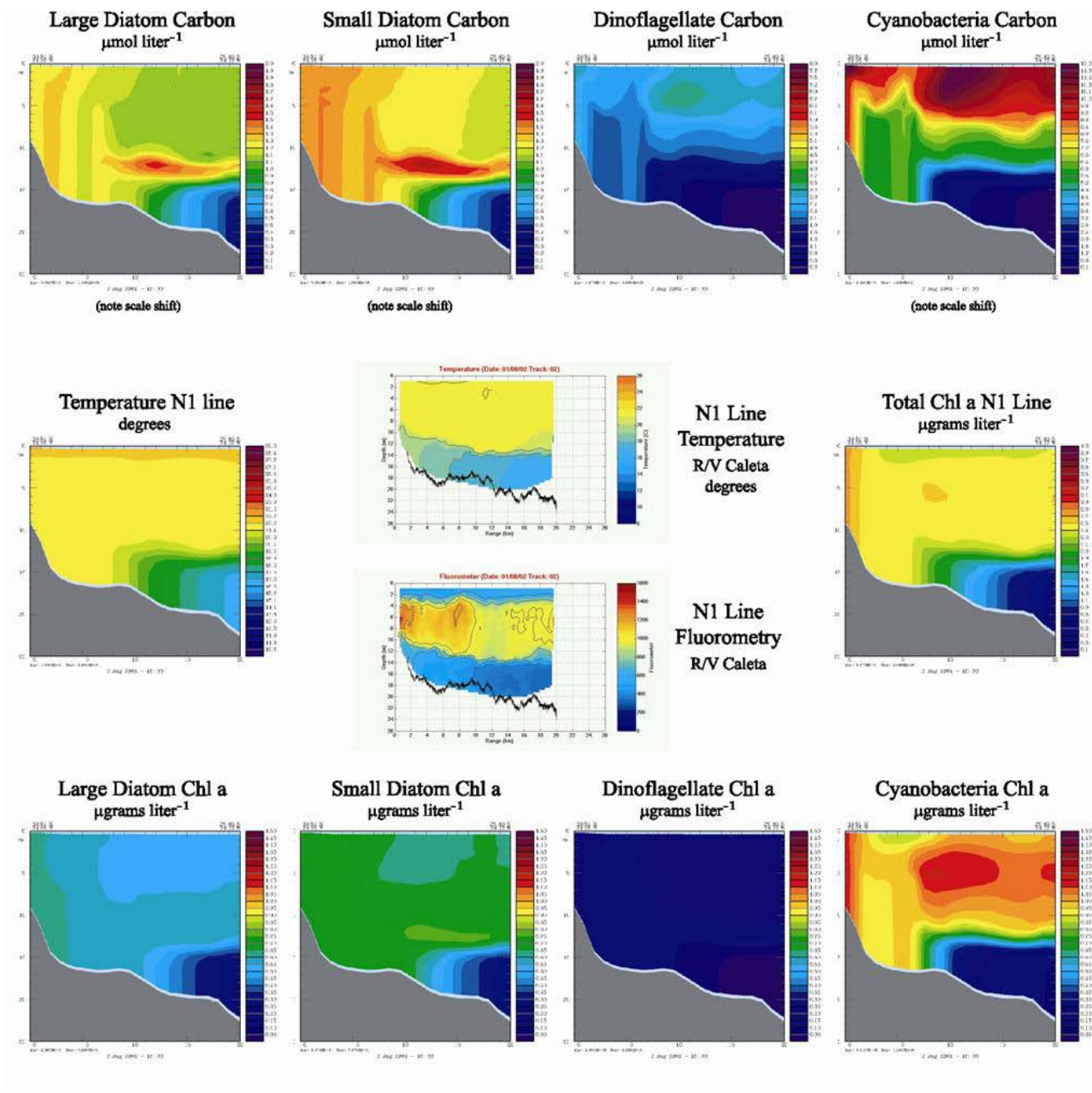
Figure 14. Vertical distribution along N1 Sampling Line of simulated carbon biomass per functional group (top row); simulated temperature, measured temperature, measured chlorophyll fluorometry, and simulated Total Chlorophyll (middle row); and simulated chlorophyll a per functional group (bottom row) at the LEO 15 field site on August 2nd during HyCODE 2001 experiment.

WORK COMPLETED – FY 2004

Field Data
The Long Term Ecological Observatory LEO-15 experiment during the summer of 2001 on the New Jersey coast was the target of hyperspectral imagery collected on three airborne platforms: PHILLS1, PHILLS2, and AVIRIS. The sensors were flown at the respective altitudes of 200m, 10km, and 20km. Atmospheric path radiance accounts for the majority of the radiance seen by airborne sensors over oceanographic scenes, and a suite of ground-based sun photometers were employed during this field effort to help characterize one of the largest unknown contributors to the path radiance, the aerosol component. The primary instrument was an automated sun radiometer ASR located at the Rutgers University Marine Field Station, the command post for the experiment. Additional handheld sun photometers (Microtops) were deployed at adjacent land targets and on small research vessels in nearshore waters. Two versions of the Microtops were employed, one for aerosols and one for ozone. Downwelling irradiance (E_d) was collected by a pair of automated Licor 1800 radiometers which were programmed and synchronized to collect every 10 or 15 minutes. Additional meteorological measurements were made to characterize the atmospheric conditions.

For this effort, we used the atmospheric correction algorithm, TAFKAA, a lookup table correction based on a modification of a vector radiative transfer code (Ahmad and Fraser, 1982). The TAFKAA code was generated using many subroutines from Gao's ATREM for geometry, solar, spectral, and water vapor (Gao and Davis, 1997; Gao et al., 2000; Montes et al., 2001). Accurate remote sensing reflectance (R_{rs}) values were the overriding goal of this effort, not atmospheric products. The accuracy of these is important to the ability to compare the imagery and imagery products (eg. chl_a, k490, CDOM) from all the HSI platforms as well as MODIS and SEAWIFS.

ROMS/EcoSim
The ROMS 2.0 version was scrapped before it was widely distributed. The physical circulation modeling group at Rutgers University moved to release ROMS v2.1. The EcoSim 2.0 subroutines were recoded once again to use the ROMS v2.1 code. In addition, it was determined that the previous use of the RADTRAN spectral irradiance code (Gregg and Carder, 1990), which was used in an off-line mode, was no longer supportable by the ROMS development team. The ingestion of large files caused significant I/O delays in the parallelization of code. The entire RADTRAN code, as well as the EcoSim 2.0 subroutines had to be recoded for the ROMS v2.1 before we could run within the latest NJB simulations.

During this recoding, a pseudo 1-D version of ROMS v2.1 (called BIO_TOY) was created to distribute and debug ecological codes that were designed to run within the ROMS code set. The pseudo 1-D version was actually a full 3-D 6x6 matrix with periodic boundary conditions. This development allowed for debugging as well as distribution of ROMS/EcoSim to others interested in developing the ROMS/EcoSim code.

RESULTS – FY2004

Field Data
Situated on the mid-Atlantic coast about 250km south of New York City, the summer frontal passages at LEO15 are typified by strong surface wind shifts. Dominant winds are from the southwest prior to the front, switching to the NE immediately after. For brief periods immediately following the fronts, the sky conditions were favorable for collection of remote spectral imagery. There were frontal

passages on July 20th, 24th, 26th, and 29th. Sun photometry was concentrated on the date with associated hyperspectral overflights: July 21st, 23rd, 27th, 31st, and August 1st, and 2nd. A summary of all the measured atmospheric parameters is included in Table 3.

Table 3. Atmospheric Parameters from LEO-15 during AM/PM Flight Windows

July	am pm	$\tau_{a\,550}$ ASR	$\tau_{a\,550}$ Mtops	α ASR	O3 µtops	WV µtops	Rel Hum	Winds Dir-m/s	Press mbar	Air °C
21	a	0.09		1.6-1.7	324	1.0	48	348°-2.3	1019	23.5
21	p	0.08		1.4-1.6	326	0.9	61	157°-4.6	1018	22.9
23	p	0.13	0.113-0.184	1.7-1.8	317	1.9	85	188°-8.3	1018	24.0
27	a	0.05		0.9	324	0.7	57	046°-7.6	1026	19.9
27	p		0.084-0.176	0.8-0.9	320	0.6	48	087°-4.0	1024	20.2
31	a	0.10	0.122-0.153	1.3-1.4	324	1.3	60	035°-3.6	1026	21.3
31	p	0.17		1.6	330	1.6	64	127°-4.3	1026	21.2
Aug										
1	a	0.14	0.146-0.177	1.6	320	1.6	67	249°-1.2	1030	21.1
1	p	0.19		1.9-2.0	325	1.8	45	217°-7.8	1028	26.6
2	a	0.22	0.198-0.325	1.9	309	1.5	62	270°-2.9	1029	23.6

There were two distinct aerosol characteristics at LEO associated with the frontal passages. Before the July 26th front, the typical conditions for $\tau_a \sim 0.1$-0.2 and $\alpha \sim 1.5$-1.8. Immediately following the storm (July 27th), τ_a dropped to exceptionally low values of 0.07-0.1 with $\alpha \sim 1.2$-1.3. These were consistent throughout the day, but they were masked in the ASR products by the formation of high altitude jet contrails (data not shown). The larger storm event on July 29-30th produced a similarly clear atmosphere on July 31st. However, it degraded rapidly during the morning. The τ_a climbed steadily throughout the next 60 hours from the lowest to highest values of the experiment. Meanwhile, the α increased from 1 to 2 which is indicative of a switch from smaller urban aerosols to more maritime with higher humidity.

Due to the low aerosol loading, July 27th would have been the best day for hyperspectral imagery. However, the temperature and water vapor conditions were favorable for the formation of contrails by high altitude aircraft. These contrails obscured the sun for most of the morning flight window, the 40-50° solar zenith angle. These clouds were relatively thin by the time they crossed the sun such that the ASR processing algorithm did not screen them from the data set. The effect is shown as a diminution

in E_d and spikes in the τ_a and α. Therefore, the majority of the effort to date has concentrated on imagery from July 31st, 2001.

Atmospheric correction of all remote sensing platforms has always been a challenging task. In oligotrophic waters, the traditional method of atmospheric correction has been to attribute all NIR sensor radiance to path radiance and use it as an offset throughout the visible range (dark NIR, Gordon and Morel, 1983). In coastal ocean waters, this is not possible as suspended sediments, bottom reflectance, macrophytes, and phytoplankton blooms contribute to the NIR signal; necessitating a better characterization of the path radiance. An alternative to the dark pixel method is to acquire coincident atmospheric measurements on the sea surface (or near-by) and directly calculate the path scattered radiance. In this approach, the sea truth data is used for validation, and/or iteratively used to fix the atmospheric parameters over the scene to provide the best match to the measured sea surface data. Because the LEO data set includes sea truth measurement, as well as sunphotometer and atmospheric measurements, it provided an excellent demonstration of the capabilities of each of these approaches. The AVIRIS data set was selected for this demonstration because it provides a midpoint in the ground spatial resolution between the high resolution PHILLS and the satellite imagery. Also, it was believed that the NIR bands of AVIRIS (which sampled out past >2 µm) would be more likely to be used as dark pixel values than the PHILLS which is limited in the long wavelengths to about 900 nm.

To see the differences that these approaches have on coastal imagery, it is necessary to look at individual AVIRIS scenes as opposed to an entire flight line or image mosaic. Two scenes, one inshore and the other offshore (Figure 15) were selected from the AVIRIS line over the Rutgers field station. The Fixed atmosphere and aerosol parameter set clearly retrieves a better correction of this coastal environment. In shore, the bottom features in the water are clearly distinguishable and recognizable (Figure 15a). Offshore, we see the impact of surface glint in the wave patterns on the surface, and a bloom of brighter material in the upper right of the scene (Figure 15b). In addition, there is a boat in the middle of this image, which is followed by a long wake. This is contrasted with the dark-NIR approach (Figure 15c and 15d). The inshore image confuses many of the bottom features with aerosols and atmospheric effects, and removes these features from the scene (Note the land is masked using an NDVI method, which is required to use the dark-NIR approach. These masked areas are shown in purple). The offshore scene has similar problems as much of the wave features are confused with aerosol and atmospheric properties. In addition, the boat and its wake are removed from the image. These data and analysis clear demonstrate the errors associated with automated atmospheric removal based on a dark-NIR approach.
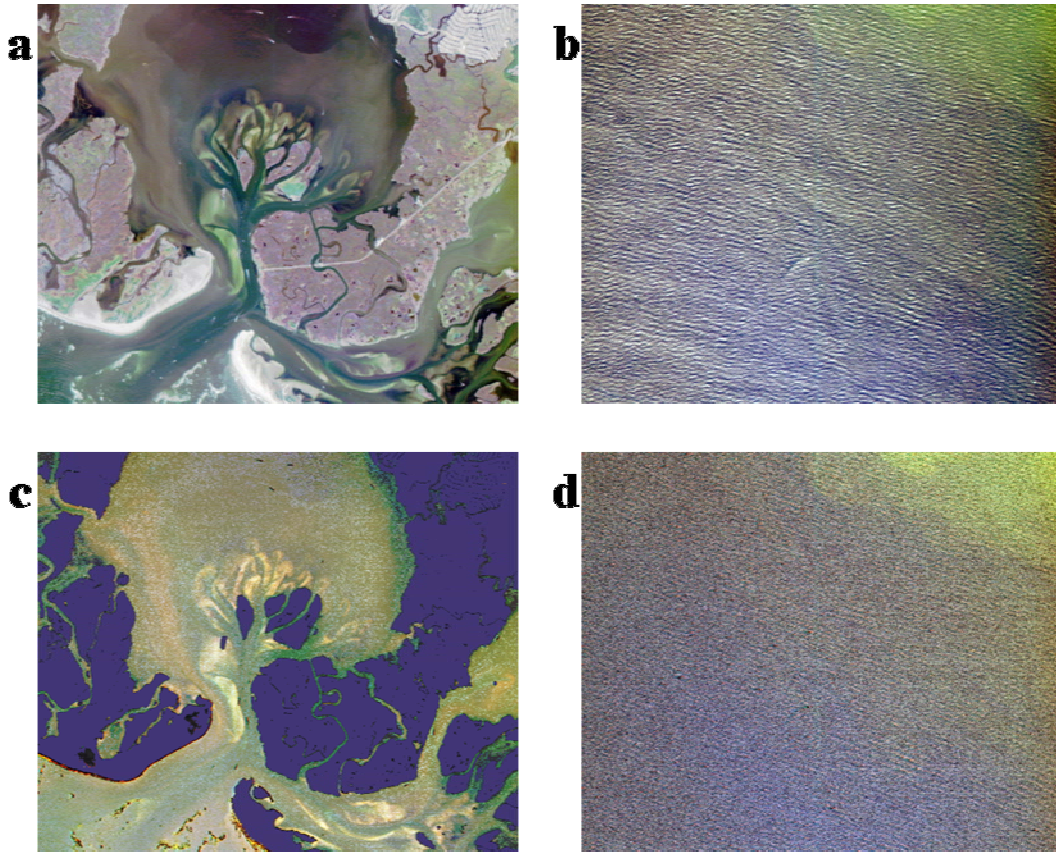
Figure 15. Atmospheric correction of AVIRIS scenes Inshore and Offshore on July 31, 2001. (a) Inshore, atmospherically corrected image using measured atmosphere and aerosol data, (b) Offshore atmospherically corrected image using measured atmosphere and aerosol data, (c) Inshore, atmospherically corrected image using dark-NIR approach, and (d) Offshore, atmospherically corrected image using dark-NIR approach. The fixed approach using measured data clearly shows a better retrieve of subsurface and surface features in these coastal waters with high NIR reflectance than does the atmospheric correction using a dark-NIR assumption.

ROMS/EcoSim
The recoding of the EcoSim and RADTRAN routines into ROMS v2.1 was successful, as the BIO_TOY results (Figure 16) demonstrate. The next physical circulation model runs are being generated for the apex region of the New Jersey/New York Bight. We want to run concurrent with this next set physical runs.
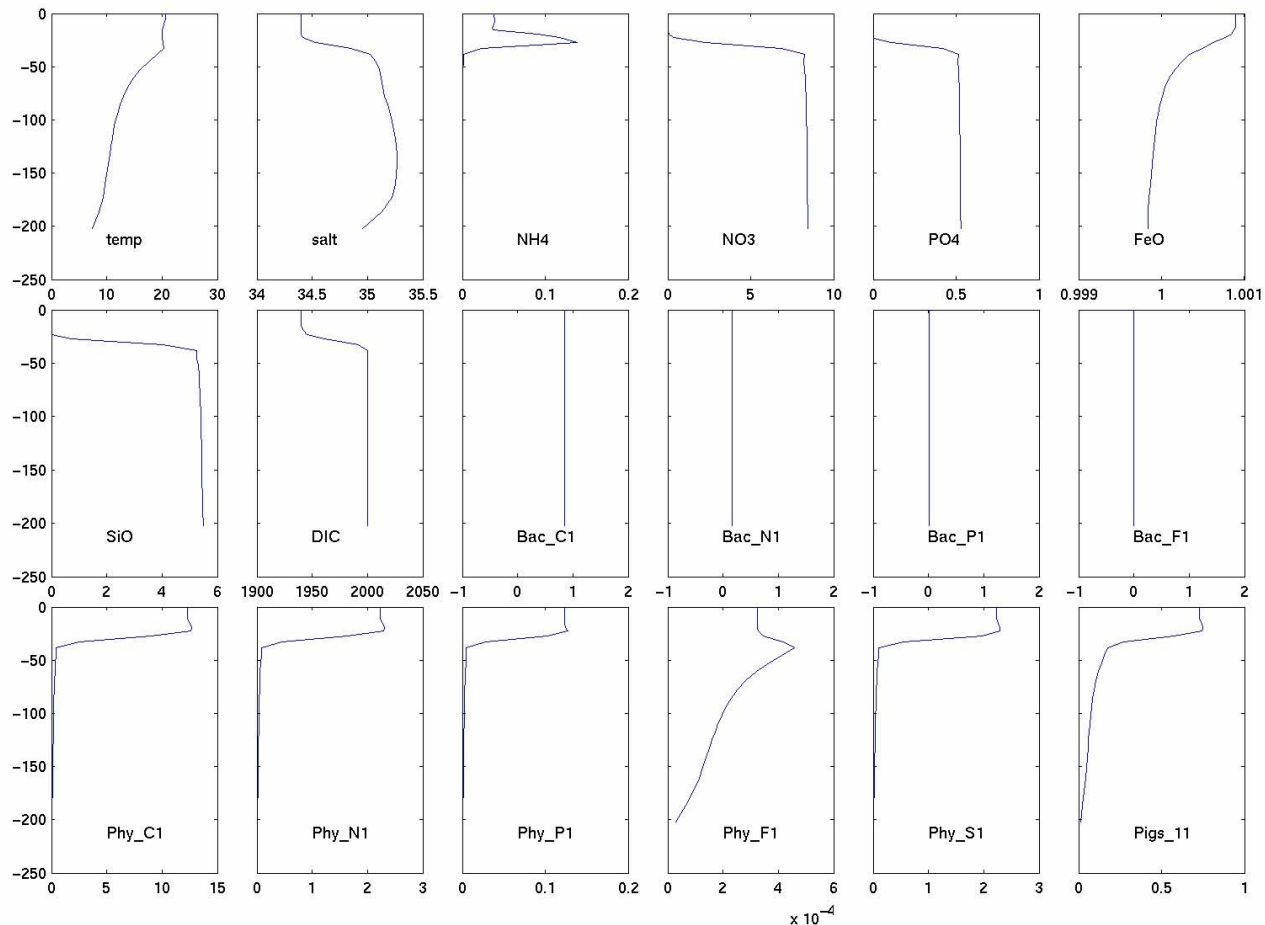
Figure 16. Pseudo 1-D results from ROMS/EcoSim v2.1 code, with full spectral irradiance built into the ROMS code set.

WORK COMPLETED – FY 2005

This last 3 months marked the wind up of this HyCODE work. Our work at FERI was multifaceted, including interacting with other HyCODE participants at LEO-15, West Florida Shelf, and COBOP sites. The remote sensing aspects of this program were very successful, leading to numerous publications, as well as continuing programs in hyperspectral remote sensing. These programs pursue both 6.1 basic research and 6.2 applications research (see ONR Programs of C. Mobley, W. Bissett, and D. Kohler), as well as generating support from other agencies (e.g. NOAA). Our interactions with the group have also helped with the development of new satellite remote sensing sampling techniques and analytical techniques (see publication list). In this capacity, we served as team members adding knowledge and skills to the overall HyCODE effort.

The modeling effort progressed well, but not to the same degree as the remote sensing. The ROMS v2.1 was updated. However, the modeling team rapidly began making changes to the code that were irreversible and once a simulation was completed, the physical code was discarded. We tried to run v2.1 3-D simulations, whose physical modeling efforts were funded by two different programs (ONR Coupled Boundary Layers/Air-Sea Transfer, CBLAST, and NSF Lagrangian Transport &

Transformation Experiment, LaTTE). However, the versions of the ROMS code for each of these programs were not compatible with the EcoSim subroutines. In one case, the CBLAST code was a unique subset of the ROMS v2.1 that was discarded once the experiment was completed. In the LaTTE case, the ROMS code used in the simulation was another unique subset of the v2.0 code, and the EcoSim v2.1 code was not backwards compatible. In addition, during the first quarter of FY 2005 we were informed that we would have to once again update the EcoSim subroutines to version 2.3 if we wished to continue in the ROMS development path, as well as hope to generate 3-D solutions for the NJB in the Spring of 2005.

While we have demonstrated the coupling of ecology and optics in a 3-D numerical simulation, the results demonstrated errors in the physical code rather then allow us to advance the original goals of the 5-10 day operational optical forecast (see FY 2002). The reasons for the slower than expected development revolve mainly around the engineering requirements for the physical modeling effort. The computational engineering of a physical nowcast/forecast system appears to be much harder than anyone had anticipated. The ROMS code set is probably one of the most advanced efforts to date at trying to generate a community model for ocean circulation modeling. Unfortunately, the physical modeling in the community is far closer to proto-type development rather than a robust engineering effort that may be used as a foundation for advanced ecological and optical applications.

To accurately resolve the non-linear time-dependent ecological and optical processes in a short-term numerical simulation requires a nearly perfect physical simulation. This requirement results from fact that the problems and errors seen in the non-conservative tracers (phytoplankton, CDOM, sediments, etc.) in a numerical simulation are directly related to the time scale of interest at which those tracers are studied. For 5-10 day forecasts, the 0th-order problem is accurate initialization of all of the ecological and optical tracer fields. A successful initialization of the model also includes the initialization of the boundary conditions of the region of interest. Following this, the 1st-order problem is the successful prediction of the advective fluxes of the tracers. If the advective fluxes are strong enough to dominate the signal in the region of interest, then the solution must be accurate at the boundaries as well as in the model domain. Lastly, the time-dependent change in ecology and optics is a 2nd-order order problem, which requires that the 0th- and 1st-order problems are reasonably solved and accurate. If these are not adequately solved then the errors in their solutions are likely to overwhelm the errors in the ecological and optical equations.

One solution that circulation modelers use to overcome the difficulties in initial conditions and numerical coding is to assimilate hydrodynamic data. Unfortunately, this tends to change the mass fields of temperature and salinity without respect to the time history of the tracers associated with those mass fields. These changes to the model's hydrodynamic fields reflect real errors in the model code and initialization, and these errors will continue to propagate throughout the model domain in the mass tracer fields, as well as in the tracer's non-linear, time-dependent change calculations. As has been demonstrated in this effort, it is possible to over constrain a poor physical model with real data such that realistic short-term forecasts are generated; yet, the process of assimilation does not address the real problems associated with inaccurate initial state conditions, or the errors inherent in the hydrostatic approximation equations. While assimilation may solve the operational problem of advective forecasts, it is unclear that they will be the panacea to solving the operational forecast of time-dependent change of ecological and optical tracers in the coastal zone. In addition, the continued focus on assimilation as the means to solve the physical problems may actually slow the development of the ecological and optical models, for assimilation efforts seeks to "fix" problems by forcing the physical simulation to match the data, rather than focusing on the fundamental processes driving the

circulation. Any errors which are propagating in the model equations or initial state, will drive errors in the time-dependent change in the ecological and optical tracers. Forcing the hydrodynamic fields without regard to the non-conservative tracers will yield poor quantitative simulation results for these tracers.

The ROMS/EcoSim code works, and as in the v2.1, it will be available in the v2.3 release of the ROMS/TOMS modeling code set. As an open source code, this is a boon for the community of users who may wish to explore optical and ecological interactions without having to start from scratch in the development of optical forecast modeling. We have also demonstrated the value of coupling optics and ecology to advanced circulation models, in particular by showing the far field impacts of poorly constrained assimilations of physical data on the non-conservative optical and ecological tracers. This feedback between physical and optical simulations will allow for better predictions of each in future coastal nowcast/forecast systems. Further development into a transitionable code will require a large dedicated that makes stakeholders out of the physical modeling community. They must see the value in simulating the circulation of non-conservative tracers in a robust stable numerical environment. For such to occur, 1) the physical model must become easier to use and less restrictive in its user-specified application, and 2) a convincing case must be made that inclusion of non-conservative tracers in a coastal ocean nowcast/forecast system is an important effort. If there was a failure on our part in this effort, it was that we were unable to make this convincing case. It may have been that the state of the physical code was just not ready to attempt more advanced predictive modeling of 2nd-order effects. This statement in no way should be seen as a lack of effort, but rather just that the problem may have been more difficult than anyone anticipated.

IMPACTS/APPLICATIONS

The abilities to identify bathymetry, submerged obstacles, bottom type, or water clarity are clearly required for Mine Warfare (MIW), Mine Counter Measures (MCM), and Naval Special Warfare (NSW), particularly in the Very Shallow Water (VSW), riverine and estuarine environments. These requirements may be satisfied by 1) in-water systems that measure the properties of interest directly, i.e. multibeam sonar and laser-line scanners, 2) estimates from inversion of remote sensing data, or 3) forecasts from 4-D environmental models. The focus on optical measures rather than acoustic measures allows for the estimation of these environmental characterizations, and target detection (e.g. Mine-Like Objects for MCM), from larger stand-off distances in access denied areas via remote sensing on aircraft and spacecraft platforms. Optical properties are also well suited for rapid environmental assessment, as the instrumentation to measure absorption, attenuation, and water-leaving radiance are better engineered and more stable than those systems to determine chlorophyll biomass, which has been a traditional proxy for optical clarity. In addition to the Naval uses, optics could become a better proxy for coastal resource managers, since these parameters can be more quantitatively described, with instrumentation that is more robust. Thus, sampling and modeling of the optical properties of the coastal zone would be a boon to environmental resource managers, as well as those Naval operations that depend upon water clarity, bathymetry, bottom typing, target detection, and performance prediction modeling.

RELATED PROJECTS

The list of HyCODE PI's is extensive and can be found at http://www.opl.ucsb.edu/hycode.html.

REFERENCES

Ahmad, Z. and Fraser, R.S., 1982. An iterative radiative transfer code for ocean-atmosphere systems. Journal of Atmospheric Science, 39: 656-665.

Arango, H.G., Bissett, W.P., Glenn, S.M. and Schofield, O.M., 2002. Coupled Physical/Bio-Optical Model Experiments at LEO-15, AGU/ASLO Ocean Sciences, Honolulu, HI.

Austin, R.W. and Petzold, T.J., 1981. The Determination of the Diffuse Attenuation Coefficient of Sea Water Using the Coastal Zone Color Scanner. Oceanography from Space. Plenum Press, New York, NY, U. S. A., 239-256 pp.

Biggar, S.F., 1998. Calibration of a visible and near-infrared portable transer radiometer. Metrologia, 35: 701-706.

Bissett, W.P., Carder, K.L., Walsh, J.J. and Dieterle, D.A., 1999a. Carbon cycling in the upper waters of the Sargasso Sea: II. Numerical simulation of apparent and inherent optical properties. Deep-Sea Research I, 46(2): 271-317.

Bissett, W.P., Walsh, J.J., Dieterle, D.A. and Carder, K.L., 1999b. Carbon cycling in the upper waters of the Sargasso Sea: I. Numerical simulation of differential carbon and nitrogen fluxes. Deep-Sea Research I, 46(2): 205-269.

Gao, B.-C. and Davis, C.O., 1997. Development of a line by line based atmosphere removal algorithm for airborne and spaceborne imaging spectrometers. In: M.R. Descour and S.S. Shen (Editors), Imaging Spectrometry III. SPIE 3118, pp. 322-329.

Gao, B.-C., Montes, M.J., Ahmad, Z. and Davis, C.O., 2000. An atmospheric correction algorithm for hyperspectral remote sensing of ocean color from space. Applied Optics, 39(6): 887-896.

Gordon, H.R. and Morel, A., 1983. Remote assessment of ocean color for interpretation of satellite visible imagery, A review. Springer-Verlag, New York, 114 pp.

Gould, R.W. and Arnone, R.A., 1998. Three-dimensional modelling of inherent optical properties in a coastal environment: coupling ocean colour imagery and *in situ* measurements. International Journal of Remote Sensing, 19(11): 2141-2159.

Gregg, W.W. and Carder, K.L., 1990. A simple spectral solar irradiance model for cloudless maritime atmospheres. Limnology and Oceanography, 35(8): 1657-1675.

Mobley, C.D., Bissett, W.P., Bowles, J.H., Davis, C.O., Downes, T.V., Gleason, A., Kohler, D.D.R., Leathers, R.A., Louchard, E.M., Montes, M.J., Reid, R.P. and Sundman, L.K., 2004. Interpretation of hyperspectral remote-sensing imagery via spectrum matching and look-up tables. Applied Optics: in press.

Montes, M.J., Gao, B.C. and Davis, C.O., 2001. A new algorithm for atmospheric correction of hyperspectral remote sensing data, in Geo-Spatial Image and Data Exploration II. In: W.E. Roper (Editor), Proceedings of SPIE, Orlando, FL, pp. 23-30.

Pope, R.M., 1993. Optical absorption of pure water and sea water using the integrating cavity absorption meter, Texas A&M University, College Station.

Pope, R.M. and Fry, E.S., 1997. Absorption spectrum (380-700nm) of pure water. II. Integrating cavity measurements. Applied Optics, 36(33): 8710-8723.

Smith, R.C. and Baker, K.S., 1981. Optical properties of the clearest natural waters (200-800nm). Applied Optics, 20(20): 177-184.

Song, Y.T. and Haidvogel, D.B., 1994. A semi-implicit ocean circulation model using a generalized topography-following coordinate system. J. Comp. Phys., 15: 228-244.

Stramski, D. and Mobley, C., 1997. Effects of microbial particles on oceanic optics: A database of single-particle optical properties. Limnol. Oceanogr., 42(3): 538-549.

Stramski, D., Reynolds, R.A., Kahru, M. and Mitchell, B.G., 1999. Estimation of particulate organic carbon in the ocean from satellite remote sensing. Science, 285: 239-242.

PUBLICATIONS

Bissett, W. P., Arnone, R., DeBra, S., Dye, D., Kirkpatrick, G., Mobley, C., and Schofield, O.M. (2005). The Integration Of Ocean Color Remote Sensing With Coastal Nowcast/Forecast Simulations Of Harmful Algal Blooms (HABs). UNESCO Monographs on Oceanographic Methodology- Manual on Harmful Marine Microalgae, UNESCO [submitted, refereed].

Mobley, C. D., L. K. Sundman, C. O. Davis, T. V. Downes, R. A. Leathers, M. J. Montes, J. H. Bowles, W. P. Bissett, D. D. R. Kohler, R. P. Reid, E. M. Louchard, and A. Gleason, 2005. Interpretation of hyperspectral remote-sensing imagery via spectrum matching and look-up tables. *Applied Optics* **44**(17), 3576-3592. [published, refereed]

Schofield, O., Bosch, J., Glenn, S., Kirkpatrick, G., Kerfoot, J., Moline, M., Oliver, M., and Bissett, P. (2005). Harmful Algal Blooms in a Dynamic Environment: How Can Optics Help The Field-Going and Sample-Poor Biologist? UNESCO Monographs on Oceanographic Methodology- Manual on Harmful Marine Microalgae, UNESCO [submitted, refereed].

Bissett, W.P., Arnone, R., DeBra, S., Deterlie, D., Dye, D., Kirkpatrick, G., Schofield, O. and Walsh, J. (2005). Predicting the Inherent Optical Properties and Colored Dissolved Organic Matter Dynamics on the West Florida Shelf. Marine Chemistry, 95, 199-233, [published, refereed].

Glenn, S., Arnone, R., Bergman, T., Bissett, P., Crowley, M., Cullen, J., Gryzmski, J., Haidvogel, D., Kohut, J., Moline, M., Oliver, M., Orrico, C., Sherrell, R., Song, T., Weidemann, A., Chant, R. and Schofield, O., 2004. The Biogeochemical Impact of Summertime Coastal Upwelling on the New Jersey Shelf. Journal of Geophysical Research: 109 (C12S04), [published, refereed].

Chen, R.F., Bissett, W.P., Coble, P., Conmy, R., G. Gardner, B., Moran, M.A., Wang, X., Wells, M.L., Whelan, P. and Zepp, R.G. (2004). Chromophoric Dissolved Organic Matter (CDOM) Source Characterization in the Louisiana Bight. Marine Chemistry, 89(1-4): 257-272, [published, refereed].

Kohler, D.D.R., Bissett, W.P., Steward, R.G. and Davis, C.O., 2004. A New Approach for the Radiometric Calibration of Spectral Imaging Systems. Optics Express, 12(11), [published, refereed].

Mobley, C.D., Stramski, D., Bissett, W.P. and Boss, E., 2004. Optical modeling of ocean waters: Is the Case 1 - Case 2 classification still useful? Oceanography, 17(2): 60-67, [published, refereed].

Oliver, M.J., Kohut, J.T., Irwin, A.J.G., Schofield, O.M., Glenn, S., Moline, M.A., and Bissett, W.P. (2004). Bioinformatic Approaches for Objective Detection of Water Masses. Journal of Geophysical Research, 109(C7): 12, [published, refereed].

Philpot, W.D., Davis, C.O., Bissett, W.P., Mobley, C., Kohler, D.D.R., Lee, Z.P., Snyder, W., Steward, R.G., Gould, R. and Arnone, R., 2004. Bottom characterization from hyperspectral image data. Oceanography, 17(2): 76-85, [published, refereed].

Schofield, O., Arnone, R., Bissett, P., Dickey, T., Davis, C., Finkel, Z., Oliver, M. and Moline, M., 2004. Watercolors in the coastal zone: what can we see? Oceanography, 17(2): 24-31, [published, refereed].

Schofield, O., Bergmann, T., Oliver, M., Moline, M., and Bissett, P. (2004). Inversion of the Bulk Absorption in the Mid-Atlantic Bight and its Utility for Water Mass Analysis in Optically Complex Coastal Waters. Journal of Geophysical Research, 190(C12S04): 12 [published, refereed].

Schofield, O., Bissett, W. P., Frazer, T.K., Iglesias-Rodriguez, D., Moline, M.A., Glenn, S. (2003). Development of Regional Coastal Ocean Observatories and the Potential Benefits to Marine Sanctuaries, Marine Technology Society Journal, 37 (1): 54-67, [published, refereed].

Shulman, I., Haddock, S.H.D., McGillicuddy, D.J.Jr., D. Paduan, J.D., Bissett, W.P. (2003). Numerical Modeling of Bioluminescence Distributions in the Coastal Ocean. Journal of Atmospheric and Oceanic Technology 20 (7):1060-1068, [published, refereed].

Zhang, X., Lewis, M., Bissett, P. and Johnson, B. (2004) Optical Influence of Ship Wakes. Applied Optics, 43(15): 3122-3132, [published, refereed].

Davis, C. O., Bissett, W. P., Brown, C. (2003). Optical remote sensing of the coastal ocean: Future directions for observing and monitoring, Earth System Monitor, Vol. 13, No. 2, [published].

Davis, C. O., J. Bowles, R. A. Leathers, D. Korwan, T. V. Downes, W. A. Snyder, W. J. Rhea, W. Chen, J. Fisher, W. P. Bissett and R. A. Reisse (2002). Ocean PHILLS hyperspectral imager: design, characterization, and calibration, Optics Express, 10(4): 210-221, [published, refereed].

Schofield, O., Bergmann, T., Bissett, W. P., Grassle, F., Haidvogel, D., Kohut, J., Moline, M., Glenn, S. (2002). Linking regional coastal observatories to provide the foundation for a national ocean observation network. Journal of Oceanic Engineering, 27(2): 146-154, [published, refereed].

Schofield, O., Glenn, S., Chant, R., Moline, M. A., Bissett, P., Haidvogel, D., and Wilkins, J. (2002). The evolution of a nearshore coastal observatory and the establishment of the New Jersey Shelf Observing System. Oceanology International 2002, [published].

Walsh J.J., Haddad, K.D., Dieterle, D.A., Weisberg, R.H., Li, Z., Yang, H., Muller-Karger, F.E., Heil, C.A., and Bissett, W.P., (2002). A numerical analysis of landfall of the 1979 red tide of Karenia brevis along the west coast of Florida. Continental Shelf Research, 22(1):15-38, [published, refereed].

Bissett, W. P, Schofield, O., Glenn, S., Cullen, J. J., Miller, W. L., Plueddemann, A. J., Mobley, C. D., (2001). Resolving the impacts and feedbacks of ocean optics on upper ocean ecology. Oceanography, 14:30-49, [published, refereed].

Walsh, J.J., B. Penta, D.A. Dieterle, and W. P. Bissett. (2001). Predictive ecological modeling of harmful algal blooms. Human Ecological Risk Assessment, 7:1369-1383, [published, refereed].

Bissett, W.P., Schofield, O., Mobley, C., Crowley, M.F., and Moline, M.A. (2000). Optical Remote Sensing Techniques in Biological Oceanography. Methods in Microbiology, Volume 30: Marine Microbiology (J.H. Paul, ed), Academic Press, London. 519-540, [published, refereed].

Bissett, W. P., J. J. Walsh, D. A. Dieterle and K. L. Carder (1999). Carbon cycling in the upper waters of the Sargasso Sea: I. Numerical simulation of differential carbon and nitrogen fluxes. Deep-Sea Research, 46(2):205-269, [published, refereed].

Bissett, W. P., K. L. Carder, J. J. Walsh and D. A. Dieterle (1999). Carbon cycling in the upper waters of the Sargasso Sea: II. Numerical simulation of apparent and inherent optical properties. Deep-Sea Research, 46(2):271-317, [published, refereed].

Schofield, O., Grzymski, J., Bissett, W.P., Kirkpatrick, G., Millie, D.F., Moline, M., and Roesler, C.S. (1999). Optical monitoring and forecasting systems for harmful algal blooms: possibility or pipe dream? Journal of Phycology, 35, 1477-1496, [published, refereed].

Walsh, J.J., D. A. Dieterle, F. E. Muller-Karger, R. Bohrer, W. P. Bissett, R. J. Varela, R. Aparicio, R. Diaz, R. Thunell, G. T. Taylor, M. I. Scranton, K. A. Fanning, and E. T. Peltzer (1999). Simulation of carbon-nitrogen cycling during spring upwelling in the Cariaco Basin. Journal of Geophysical Research, 104, 7807-7825, [published, refereed].

HONORS/AWARDS/PRIZES

Semi-Finalist, 2003 Small Business of the Year, Florida Environmental Research Institute, W. Paul Bissett, Ph.D., Executive Director, Greater Tampa Chamber of Commerce.

Finalist, 2004 Small Business of the Year, Florida Environmental Research Institute, W. Paul Bissett, Ph.D., Executive Director, Greater Tampa Chamber of Commerce.